Intelligent high-tech coating of natural biopolymer layers

Yousef Murtaja, Lubomir Lapčík, Barbora Lapčíková, Shweta Gautam, Martin Vašina, Lubomir Spanhel, Jakub Vlček

Intelligent high-tech coating of natural biopolymer layers

Yousef Murtaja[a], Lubomir Lapčík[a,b,1,*] lapcikl@seznam.cz, Barbora Lapčíková[a,b], Shweta Gautam[b,1], Martin Vašina[b,c], Lubomir Spanhel[d], Jakub Vlček[a]

[a]Palacky University in Olomouc, Department of Physical Chemistry, Faculty of Science, 17. Listopadu 12, 771 46 Olomouc, Czech Republic

[b]Tomas Bata University in Zlin, Department of Foodstuff Technology, Faculty of Technology, Nam. T.G. Masaryka 275, 762 72 Zlin, Czech Republic

[c]Department of Hydromechanics and Hydraulic Equipment, Faculty of Mechanical Engineering, VSB-Technical University of Ostrava, 17. Listopadu 15/2172, Ostrava-Poruba, 708 33 Ostrava, Czech Republic

[d]Institute of Chemical Sciences Rennes, UMR CNRS 6226, University of Rennes 1, Campus Beaulieu, Rennes, France

[*]Corresponding author.

ABSTRACT

Polymeric materials play a vital role in our daily life, but the growing concern for the environment demands economical and natural biopolymers that can be cross-linked to create technologically innovative lightweight materials. Their cellular matrix with extreme flexibility makes them highly acceptable for application prospects in material science, engineering, and biomedical applications. Furthermore, their biocompatibility, mechanical properties, and structural diversity provide a gateway to research them to form technologically important materials. In the light of the same, the review covers cellulose derivatives. The first section of the study covers the general properties and applications of cellulose and its derivatives. Then, the biopolymers are characterised based on their dielectric

[1] Authors who equally contributed as the first author.

properties, crystallinity, rheology, and mechanical properties. An in-depth analysis of the diffuse process of swelling and dissolution followed by a brief discussion on diffusion and diffusion of crosslinking has been done. The review also covers a section on swelling and swelling kinetics of carboxymethyl cellulose (CMC) and hydroxyethyl cellulose (HEC). The examination of all the aforementioned parameters gives an insight into the future aspects of the biopolymers. Lastly, the study briefly covers some preferred choices of cross-linking agents and their effect on the biopolymers.

Keywords
biopolymers; crosslinking; diffusion coefficient; hydrogel swelling; thermodynamics

1. Introduction

The technology of intelligent materials paves way for the development of sustainable products via their acute flexibility. Their ability to adapt to environment changes in response to a stimulus, enhances their multi-functionality in daily applications as well as in all the engineering fields, medical, defence, and automobile industries. Some of the examples of intelligent materials include memory alloys, hydrogels, thermochromic pigments, photochromic pigments, biopolymer coatings, shape memory polymer etc. [1]. The structure-property relationships permit the significant variation of important physicochemical and biological properties, which broaden their application prospects in material science, engineering, and industrial sectors. The expeditious growth in the science and engineering sectors demands the development of novel and sustainable materials, thereby placing new requirements on material engineers to prepare highly sophisticated mono and composite systems [2].

In the field of materials, the cost and energy consumption for the preparation and processing of heavyweight building materials (mainly transport systems) is very high, thereby limiting

their scope for future applications. To avoid this, a constant search has been focused on development of lightweight polymer composites endowing excellent mechanical properties by using low-cost and straightforward synthesis processes. It is also worth mentioning the increasing demand to reduce the environmental wastage and carbon footprint, particularly in the materials industries. Therefore, it is required by researchers to focus on enhancing the properties and functions of the biopolymers. In the view of the same, significant research has been done to produce biopolymers and bio-composites with comparable properties and functionalities to those of traditional bio-based packaging [3]. Some of the biopolymers that have been studied extensively are: Polylactic acid (PLA), polyhydroxyalkanoates (PHA) [4], starch, cellulose, pectin, chitosan among others. It is expected that in the next decade, the weight of cars will reduce to half the original weight owing to the use of lightweight biopolymer composites; consequently, reducing the fuel consumption by 50%. The advantages of lightweight polymer composites and polymer-based ceramics will be applied further to design and manufacture advanced lightweight engines. In this context, natural biopolymers have been drawing more attention because of the following reasons: (i) construction of living organisms´ bodies can be done strategically; (ii) different properties in solid, semi-solid, and solution phases; (iii) can be applied directly without requirement of further processing; (iv) permitting the simple design of thin coatings on the surface of solids by the existing methods, which are conventional in printing arts, textile, and packaging material industries [5, 6] and thus improving hydrophobicity and hydrophilicity. Cross-linked hydrogel coatings for surface enhancement of contact lenses have also been reported [7, 8]. The literature analysis indicates a dominant position of carbon based polymers in the form of nanoscale fibres and dispersions, cyclic fullerenes, alongside silicon and boron polymers. Of the aforementioned biopolymers, the review highlights cellulose and its derivatives viz, oxycellulose, carboxymethyl cellulose, nitrocellulose and hydroxyethyl cellulose.

Cellulose is the most plentiful, renewable, and natural polymer on the planet, with yearly output ranging from 75 to 100 billion tonnes for various industrial and biological uses [9]. It is a glucose-based linear polysaccharide that gives mechanical support to plant cells, bacteria, algae, and fungi (Fig. 1(a)) [10]. Most commercial cellulose fibres are obtained as pulp (natural fibres) or derivative from the natural cellulose of wood, barks, cotton, leaves, and jute. Carboxymethyl cellulose (CMC) was the first cellulose (Fig. 1(b)) to attain commercial and industrial relevance in the 1920s, and it will continue to have a dominant position in the global market. CMC can be easily made via simple processes and low-cost ingredients. The vast market potential of CMC is the main advantage compared to other cellulose derivatives. CMC is used in the paper, textile, pharmaceutical, cosmetic, and food industries, just like cellulose and other cellulose derivatives. Nitrocellulose (NC) is also one of the most commercially relevant and widely utilized natural cellulose derivatives [11]. Its nitrogen content determines the properties and applications of NC. NC with nitrogen content below 12.0 wt% can be used for coatings, printing inks, varnishes, filtration membranes, microfluidic technology, immunoassays, and biochemical analyses [12, 13, 14]. The formation of NC aerogel significantly increases NC's surface area and broadens its applications in separations, purification science, and biomedicine [15]. Oxycellulose (OC) is a semi-synthetic derivative of cellulose that undergoes chemical depolymerization and enzymatic hydrolysis under in vivo conditions [16, 17]. It is a non-toxic, biodegradable, biocompatible, and bioresorbable polymer [18, 19]. It is a well-established surgical material commercially available as a knitted fabric or staple fibres used to stop bleeding and prevent undesirable tissue adhesion during post operative healing [20]. Hydroxyethyl cellulose (HEC) is non-ionic, hydrophilic, tasteless, and non-toxic cellulose derivative used extensively in pharmaceuticals, cosmetics, and food products (Fig. 1(c)) [21, 22]. For instance, HEC cross-linked with citric acid is used as probiotic entrapment material [23]. HEC coatings in

combination with other polysaccharides such as chitosan are used and seldom investigated [24]. It has excellent film-forming ability, biocompatibility, and biodegradability, making it suitable for biomedical applications [25]. Composites of natural biopolymers with aluminosilicates are used as packaging materials in the food industry [26].

The primary aim of this review is to characterize the aforementioned biopolymers (particularly CMC and HEC) followed by an extensive evaluation of their diffusion and diffuse process of swelling and dissolution of polymers. The review briefly covers the diffusion and coefficient or cross-linking of biopolymers, followed by a meticulous focus on mechanical properties, surface tension for spreading, diffusion coefficient, kinetics, and thermodynamics of diffusion, swelling, and dissolution [27]. The review also evaluates the preparation of varieties of industrial auxiliaries for printing arts and textile industries, such as offset print humidifying solutions, offset printing plate's protective solutions, and means for improving colouring of textiles [28, 29, 30].

2. Characterisation of biopolymers

The characterisation evaluation of biopolymers (CMC and HEC) was conducted on the basis of crystal/solid-state and liquid/cross-linked state. The dynamics of the macromolecular chain movement was studied by temperature-dependent dielectric spectra in the frequency range of 20 Hz to 1 MHz [31] (Table 1) [32]. The characterisation of CMC with corn starch on the basis of crystallinity, mean length, percent purity and mean width was also reviewed (Table 2) [33]. The data indicates the use of CMC biopolymer as a thickener, emulsion binder, and stabilizer [32, 34] in the detergent, cosmetic [35], food, pharmaceutical, drilling, and textile industries [36]. It can also act as a binding granule to form drug tablets in the pharmaceutical industries. The degree of substitution does not affect the percentage of purity.

The percentage of crystallinity varies directly with the mean width [37]. HEC is a non-ionic cellulose ether whose water solution properties are very useful in the pharmaceutical, alimentary, and industrial fields [38]. HEC can be used as thickening agent, protective colloid, binder, stabiliser, and suspending agent in a variety of industrial applications including pharmaceuticals, textiles, paper, adhesives, coatings and emulsion polymerisation [39].

Sodium salt of carboxymethyl cellulose (NaCMC) is the most extensively used CMC polymer. The rheological analysis for NaCMC indicated that the degree of substitution (DS) affects the flow properties of NaCMC samples. At higher concentration, heterogeneously substituted samples have the ability to form gels [40] and may present thixotropic or shear aging [40, 41]. As the DS decreases below a certain threshold (around 0.9), the interchain aggregates and formation of fringed micelles with crystalline core takes place [40, 42, 43, 44]. These micelles are responsible for the thixotropic and gelling properties of the weakly substituted NaCMC. The rheological properties of the physical gels of CMC without the addition of cross-linking agents depends on hydrophobic interactions between individual macromolecular chains [45, 46, 47]. This study revealed that CMC samples with DS $\approx$ 0.7-0.8 can be separated into two fractions by centrifugation. Fraction A displayed pseudo-plastic, non-thixotropic and non-gelling behaviour in salt free aqueous solution whereas fraction B displayed some solubility in water and good solubility in concentrated NaOH. The substituent distribution of fraction B was heterogeneous which led to the formation of thixotropic gel at higher concentration by hydrophobic inter-chain associations. The rheological properties of aqueous solution of HEC can be controlled by modifying the polymer backbone with side chain achievements such as ionic or hydrophobic groups [48]. In hydrophobically modified HEC [49, 50, 51], the thickening action is caused by the association of the hydrophobic side chains into an intermolecular transient network. On the

other hand, cationically modified HEC tend to behave like typical poly-electrolytes [52]. The viscosity enhancement is due to repulsion of the charged groups along the chain which expands the macromolecule. As the surfactant concentration increases, the number of side chains per micelle decreases to the point that intermolecular associations of polymer molecules are inhibited due to the electrostatic repulsion between attached micellar aggregates. As a consequence, the shear viscosity of the solution reaches a maximum and then decreases as surfactant concentration is further increased [53, 54]. The inhibition of interchain interactions through hydrophobic side chains eventually might lead to a viscosity that is even lower than that of the pure polymer solution.

Tensile strength (TS) is the film's retainable maximum tensile force. It explains the film's maximum force occurring during measurement. Various ratios of CMC produce different tensile strength results. In general, the tensile strength values reduce with the addition of a substrate. In a study conducted on CMC produced by carboxymethylation using sodium monochloroacetate and varying concentrations of sodium hydroxide, it was found that the NaOH concentration affected the TS but not the elongation at break (EB) of the CMC films [55]. TS increased with NaOH concentrations of 20 and 30 g/100 mL (Table 3) [55]. Beyond the 30 g/100 mL concentration, the TS of the films decreased. The more carboxymethyl groups there are, which is directly related to the DS, the more the inter-molecular forces between the polymer chains increased, resulting in a higher TS. Somewhat similar results for TS and EB were recorded in another studies [56, 57]. The studies involved the formation of films with CMC and corn starch. It was found that combining four grams of CMC in the absence of corn starch yielded the highest tensile strength whereas, combination of corn starch with CMC in the ratio of 3:1 yielded the lowest tensile strength (Fig. 2). The percent of elongation increased with a lower concentration of CMC-corn starch (Fig. 3). In general, it was found that the tensile strength reduces with increase in the percentage

elongation [57]. Similar results for tensile strength and elongation at break analysis of HEC were studied [58, 59, 60]. The study evaluated the tensile strength and elongation at break for pure HEC films vs the films prepared with the addition of cellulose nanocrystals (CNC). The addition of 4% of CNC increased the tensile strength by 120.2% but beyond 8%, the addition of CNC did not enhance the tensile strength. The elongation at break reduced by 95.6% in comparison to pure HEC film. The results indicated that the addition of CNC can improve the tensile strength but beyond a threshold value, the elongation at break decreases [58].

3. Diffusion of polymers and surface tension

The term ‘diffuse actions’ is understood as whole processes that include the transport of substances because of the gradients in chemical potential. Temperature, pressure, electric potential, and magnetic field have significant contributions to chemical potential gradients. Many authors have comprehensively studied this topic [34, 61, 62].

Two direct relations for explaining the diffusion phenomena are known as Fick's laws. For binary system applying the one-dimensional diffusion Fick's laws:

i. Fick´s law: $J_i = -D_i \frac{\delta c_i}{\delta x}$ (1)

ii. Fick´s law: $\frac{\delta c_i}{\delta t} = \frac{\delta}{\delta x}\left(D_i \frac{\delta c_i}{\delta x}\right)$ (2)

where t, x, J_i, D_i, and c_i are time, coordinates, diffusion flow, diffusion coefficient, and concentration of component i, respectively. For known initial and peripheral conditions by solving the given differential equations, the value of diffusion coefficient (D_i) can be determined. For unit concentration gradient, diffusion coefficient determines the flow of a substance per unit area perpendicular to the direction of flow. The values of diffusion

coefficient for low molecular weight polymers are within 10^{-5} to 10^{-14} cm^2 s^{-1}. R. M. Barrer et al. [63] divided the systems of polymer-penetrant into four different categories:

a) $\frac{\partial c}{\partial t} = D\frac{\partial^2 c}{\partial x^2}$ D = const. $c = k.c^{'}$ (3)

b) $\frac{\partial c}{\partial t} = \frac{\partial}{\partial x}\left[D(c)\frac{\partial c}{\partial x}\right]$ D = *f* (c) $c = k.c^{'}$ (4)

c) $\frac{\partial c}{\partial t} = \frac{\partial}{\partial x}\left[D(c)\frac{\partial c}{\partial x}\right]$ D = *f* (c) c = *f* '($c^{'}$) (5)

d) $\frac{\partial C}{\partial t} = \frac{\partial}{\partial x}\left[D(c)\frac{\partial C}{\partial x}\right]$ D = *f* (c, t) c = *f* '($c^{'}$) (6)

'Category a' is typical for the diffusion of rare and most di-atomic gases in polymers at the viscoelastic state. 'Category b' describes the diffusion in systems of rubber and paraffinic hydrocarbons. 'Category c' is applicable for the diffusion of heavier hydrocarbons in rubber layers. 'Category d' is very common, and the diffusion coefficient depends on concentration and time in this category. Notably, this case involves the strong mutual interactions between chain and penetrant molecules. The mutual interactions usually lead to slow relaxations in the crystalline polymer.

Many technological fields depend on the exact knowledge of the effect of solid/liquid interface interactions on final spreading of liquid drops. The experiment observed the surfactant solutions behaviour at critical micellar concentration (CM conc × 10) (Fig. 4) [64] and water drops from the impact moment to one second after the impact [65]. All the solutions have the same process of spreading (Table 4) [64]. The surface tension is the difference between the foaming medium's surface tension, the defoamer's surface tension, and both substances interfacial tension for the spreading diffusion coefficient (*S*); thus, mathematically, we can write :

$$S = \sigma_f - \sigma_d - \sigma_{df} \quad (7)$$

where σ_f is the surface tension of the foaming medium, σ_d is the surface tension of the defoamer and σ_{df} is the interfacial tension of both substances.

The defoamer's surface tension reduction causes the spreading coefficient to become increasingly positive. The process shows the defoaming's thermodynamic tendency. Equation 3 is applicable for insoluble liquid defoamers in bulk. However, deforming effectiveness can be increased by certain dispersed hydrophobic solids. The process of spreading depends mainly on surfactants.

4. Diffuse process of swelling and dissolution of polymers

4.1. Diffuse process of swelling

The conversion of solid polymer in solution at temperatures below the second-order turning point (T_g) usually comprises swelling and dissolution processes. In the swelling process, the solvents come to introduce at the solid polymeric phase and expand the solid surface in the liquid phase. This effect is known as Kirkendahl´s effect [66]. It is the impact that leads to loosening of the polymer structure thereby enhancing the movement of macromolecular chain segments, and enhancing the activity of free volume in the system alongside the replacement polymer-polymer contacts by the polymer-solvent contacts. It results in the creation of swollen surface layer with defined thickness and structure [67]. The movement of phase interface, i.e., the interface between swollen layer and the liquid solvent is necessary to understand as its own swelling. The diffusion process of polymer dissolution has been studied in detail by Lapčik and Valko [68]. According to them, the diffusion of liquid solvents into polymer foils can be evaluated on the basis of parameters describing the formation of a surface diffusion layer. Furthermore, the polymer matrix swells due to the solvent effect resulting in the developed surface diffusion layer being donated as a surface swollen layer

(SSL) [69]. The swelling process is unsteady in nature resulting formation of the swollen surface layer.

4.2. Swollen surface layer

SSL of polymer represents interphase resistance of a given value influencing the diffusion in both directions from the interface. Ueberreiter K. and Asmussen F. [69, 70, 71, 72, 73, 74, 75] reported that SSL comprises complex structures, mostly in temperatures below T_g. Its thickness δ depends primarily on molecular weight, temperature, the kinetic-thermodynamic activity of solvent and minutely on the thermal history of polymer samples. The other four layers within SSL were reported by the authors mentioned (Fig. 5) [69, 72, 74, 76]. If the melting temperature drops below T_{gel}, i.e., $T_L < T < T_{gel}$, the rubbery layer δ_2 disappears and then only layers δ_1, δ_3, and δ_4 are retained. When melting temperature decreases below T_L, i.e., $T < T_L$, layers δ_1 and δ_3 disappear, so the SSL is formed only by layer δ_4. The latter two cases can be well clarified by the following reasons: dissolution in the range of temperatures (T_{gel}) and (T_L), i.e., $T_L < T < T_{gel}$ leads to weakening of the rubbery layer δ_2 to a value that is not visible; it indicates that it cannot affect the swelling process. The transport of solvated polymers into the coexisting liquid phase of the solvent is the rate-determining step at higher dissolution temperatures. The liquid layer consists of solvent molecules accumulated by adsorption on the surface of polymeric substances. Even if the dissolution in flowing solvent is the rate of flowing fluid in this layer virtually zero, the concentration of polymer in this layer grows from almost zero value, which is on the interface with flowing solvent at a value φ_ξ that is on the interface with the rubbery layer. The thickness of this layer depends decisively on the rate of the solvent flow. With increasing rate, the thickness decreases to a certain limit value and does not change anymore. The rubbery layer has the character of a liquid phase with a fixed structure. The content of solvent molecules is large, and the thickness of the layer is comparable with the thickness of the liquid layer. The concentration

gradient from one interface to another is almost the same as the liquid layer. A sudden increase in the concentration gradient was observed at the rubbery and tough swollen layer interface. Polymer chains in this layer do not move in the same fashion as in the liquid phase and the thickness of the layer is significantly smaller than in the previous two regions. The system of this layer is composed of the continuous liquid phase, which is continuously permeated by a dispersed polymer (with a gel-like character). The concentration of the solvent is markedly smaller compared to the rubbery phase. The infiltration layer is characteristically different from the previous. The movement of solvent molecules in the direction of concentration gradient takes place in this layer, probably in the exact mechanism as the gas transport through polymeric membrane, i.e., jumping from one vacancy to another without any significant movement of polymer segments. The number of polymer-polymer cross - links is comparable with the number in the original sample. As mentioned before, it is clear that the diffusion of solvent molecules controls the kinetics of polymers into a solid polymer sample.

5. Diffusion and diffusion coefficient of cross-linking

Diffusion involves the movement of atoms, molecules, and ions from a higher concentration region to a lower one. The concentration gradient is the major driving force of diffusion. Various fields, such as chemistry, widely use the diffusion concept to characterise swelling kinetics [77] and measurements of diffusion of macromolecules [78]. A mean square displacement's long-time slope gives the diffusion coefficient (*D*) of cross-linking:

$$D = \frac{1}{6}\mathrm{lim}_{t\to\infty}\frac{d}{dt}\langle|r(t) - r(0)|^2\rangle \quad (8)$$

where *r(0)* and *r(t)* are the centres of the mass's vectors at time = 0 and *t*, respectively, in the biopolymer CMC, an increase in the polymer concentration first reduces the diffusion coefficient. However, a larger polymer concentration than a critical value increases the

diffusion coefficient [79]. The diffusion coefficient in a CMC relates to the excess mixing volume and biopolymer fraction in the solution. Within the concerned region, the concentration of the solution density is given by the formula:

$$p = p_B^0(1+aWp) \quad (9)$$

where p_B^0 and aWp are the pure solvent density (0.998 g/cm^3) and the polymer concentration (wt/wt), respectively. For CMC, the value of "a" is 0.0047.

$$\frac{Dg}{D0} = \exp[-\pi \cdot (\frac{rs+rf}{ksa\varphi^{-0.75}C\infty^{-0.25}(1-2\chi)^{-0.253}+2rf})^2] \quad (10)$$

where a is the equivalent bond length of the monomer, φ is the polymer volume fraction, r_s is the radius of solute, r_f is the radius of polymer chain, C_∞ is the characteristic ratio of polymer, χ is the Flory-Huggins polymer/solvent interaction parameter, D_g is the diffusion coefficient of solute in gel, and D_0 is the diffusion coefficient of solute in water calculated from MD simulation and verified by literature [79]. Since the fitting parameter for the different polymers and solutes considered, Amsden proposed this model as a "universal" model for solute diffusion in hydrogels.

An increase in the cross-linking density causes the diffusion of sodium ions to reduce at 0.5 M. The dynamic and theoretical predictions helped obtain the particles' normalized diffusion [79]. The water content variation also changes the rate of diffusion [57]. There is a need to estimate the Rhodamine's rotational relaxation time to calculate the translational diffusion coefficient [79]**.** The increase in the cross-linking density causes the diffusion coefficient of small. The rise in the relaxation times of the hydrogen bonding correlates with the reduction in water diffusion.

6. The kinetics of swelling and dissolution of CMC and HEC

The swelling and dissolution mechanism for CMC and HEC are not homogeneous because of its multi-scale and complex structures. The ballooning phenomena are the most spectacular

effects of the heterogeneous swelling and dissolution. Some selected zones along the fibre provide places for swelling to take place. It is assumed that the structural origins of the ballooning effect relate to the morphological variations among the walls. Each of the balloons presents a swollen state of the biopolymers. The quality of the solvent strongly influences the swelling and dissolution mechanisms (Fig. 6) [68]. The swelling and dissolution characteristics can be revealed at the different cellulose structures' lengths from the macromolecule to the fibre's walls.

6.1. Kinetics of swelling

In practical applications, a higher swelling rate and a higher swelling capacity are required. It is well known that the swelling kinetics for the absorbents is significantly influenced by various factors such as swelling capacity, the size distribution of powder particles, specific size area, and composition of the polymer (Fig. 7, 8) (Table 5) [80, 81, 82]. Various authors [83, 84] have investigated the influence of these parameters on the swelling capacity. For example, Metz et al. [85] analysed the dependency of water absorbency of superabsorbent polymers on particle size. Results indicated that the absorption rate increased as the particle size became smaller. This may be attributed to an increase in surface area with decreasing particle size of samples [86].

In a study conducted on the formation and subsequent analysis of swelling kinetics of a CMC-N-isopropylacrylamide based hydrogel, the effect of particle size on the swelling kinetics was confirmed. The rate of water absorbance increased sharply and then began to level-off (Fig. 9) [86]. Considering the second - order kinetics, the swelling rate at any time is expressed as:

$$\frac{dW}{dt} = K(W_\infty - W)^2 \qquad (11)$$

where W is the water content of the superabsorbent at time t, W_∞ is the water content before the equilibrium has been reached and K is the constant. Substituting equation 11 with limits $t = 0$ and $W = 0$ to W, and rearrangement, the equation can be re-written as:

$$\frac{t}{W} = \frac{1}{KW_\infty^2} + \frac{1}{W_\infty}\, t \tag{12}$$

The swelling of the super-absorbent composites obeys second order kinetics (Fig. 10) [82, 86].

Similar results were found for the hydrogels developed from HEC [87]. Composite hydrogels with co-polymerization with HEC, sodium acrylate and medicinal stone (MS) were created. The analysis of kinetic swelling (Fig. 11) [87], depicted the effects of MS content, particle size and saline solution on the swelling kinetics. It was found that the swelling rate was faster at initial 600 seconds. With prolonging swelling time, the swelling rate decreased until a plateau was reached. Schott's second-order swelling kinetics model [88] (equation 13) was introduced to evaluate the hydrogels' kinetic swelling behaviours.

$$\frac{t}{Q_t} = \frac{1}{K_{is}} + \frac{1}{Q_\infty} t \tag{13}$$

were, Q_t (g/g) is the swelling capacity of the hydrogel at time t (s), Q_∞ (g/g) is the theoretical equilibrium swelling capacity, and K_{is} (g/g s) is the initial swelling rate constant.

6.2. *Kinetics of dissolution*

The dissolution of polymeric materials has some typical features. The rate of dissolution is controlled by several factors, the determining one is the diffusion rate into the polymer matrix. The diffusion rate depends on the chemical structure of the polymer, solvent and functional groups present on the polymer chain (dissolving parameter density of cohesive energy), solvent molecular volume, dissolution temperature, molecular weight of the polymer, structural ordering of the polymer etc. By getting the polymer into contact with the solvent, the diffusion of solvent molecules into the polymer matrix proceeds, creating thus

the SSL (δ) [89, 90]. The thickness of this layer depends on the temperature of dissolution, mixing rate, molecular weight of the polymer, kinetic and thermodynamic activity of the solvent, and thermal history of polymers [70, 71, 91, 92].

Surface swollen layer of a polymer represents interfacial resistance of definite matter, which influences diffusion of molecules in one or another direction from the interface. Ueberrreiter and Asmussen have found that it has a complicated structure with respect to the dissolving temperature [89].

If temperature of dissolution (T) ranges between gel point temperature (T_{gel}) and glass transition temperature (T_g) ($T_{gel} < T < T_g$), then the structure of the surface layer consists of liquid (δ_1), rubbery (δ_2), solid swollen (δ_3), and infiltration layer (δ_4). Thickness and distribution of particular layers in swollen polymer layer are represented in Fig. 12 [89].

7. Cross-linkers for creating gel-polymer

The gel in general is consisted of the cross - linked networks of hydrophilic water-soluble polymers. Gel polymers can swell after absorbing water. It is possible to prepare natural polymer-based hydrogels by mechanical and physical cross-linking [93]. In the case of polymeric networks, their structure is fully dependent on covalent bonds or physical inter-molecular interactions between individual macromolecules. However, each connecting point of the network are mutually separated by a linear secondary chain. In the case when these secondary chains are sufficiently long, and their chemical structure allows adoption of various conformations, these create soft and flexible materials. Contrary to this, rigid secondary chains cause the creation of hard and glassy materials. The characteristic property of the stable elastomeric network is its swelling ability when in contact with proper solvent systems. Therefore, because the polymeric network is, in fact, structuralised solid matter that cannot be dissolved with an exemption of the cases when there is observed loss of their

coherent macroscopic structure [65]. Thus, when such cross-linked structure is immersed into the solvent, which is miscible with the polymer chains of the network, the solvent is absorbed, and the network is swollen. The increase of the volume can be up to one thousand percent [94]. Chemical reactions initiated by pressure, heat, irradiation, and change in the pH level can facilitate cross-links formation [95]. The latter cross-linking can be achieved by chemical reactions such as polycondensation, polyaddition or by physical entanglements of macromolecular chains. Physical entanglements and disentanglements of macromolecular chains were reported [96, 97] as induced by temperature and pH of the dissolved polymer system known as helix-coil transition. For example, mixing certain chemical agents, such as cross-linking reagents with partially polymerized or unpolymerized resin creates cross-links [98]. Cross-linking is commonly used to improve starch performance for a variety of applications [99]. Cross-linking agents, such as sodium tri metaphosphate, phosphorus oxychloride, epichlorohydrin, citric acid, diphenyl sulphone, anthracene endo-peroxide [100, 101, 102], sodium tripolyphosphate, and 1,2,3,4-diepoxybutane have been used for the improvement of the materials´ mechanical properties and the starch products´ water stability.

Divinyl sulfone (DVS) is a non-zero length cross-linker that has been widely used to chemically modify polymers to improve the mechanical properties and enhance the performance according to the suitability (Fig. 13) [103]. It has been extensively used in combination with cellulose and its derivatives, especially in the pharmaceutical industries. The concentration of DVS added to the biopolymer directly influences its rheological properties. It has been found that higher concentrations of DVS increases the viscosity thereby indicating a higher cross-linking in the biopolymer [104].

Polymers may act as a basic building component of the larger systems namely of block co-polymers and micelles. The latter micelles can be organised in the presence of the surface-active agents to liquid crystalline systems [105].

8. Conclusions

Viewing the state of polymeric materials, the reviewed biopolymers possess enhanced structural diversity, biodegradability, thin coat-forming ability, and diverse flexibility, allowing them to be used in varied application prospects in technologically influential intelligent applications. The lightweight and biocompatibility of cellulose derivatives have been essential in biomedical and non-biomedical fields. The reviewed biopolymers have a high potential in the preparation of intelligent high-tech materials and in unlocking new possibilities for natural biopolymer layers to be better suited to the environment and the needs of end-users. This review provides an attractive route for the scientific community to research the technologically important and intelligent coatings for varied purposes.

Declaration of competing interest

The authors declare that they have no known competing financial interests or personal relationships that could have influenced the work reported in this paper.

Acknowledgement

The authors would like to express their gratitude for financing this research by the internal grant of Palacky University in Olomouc (project no. IGA_PrF_2022_020) and to the internal grant of Tomas Bata University in Zlin (project no. IGA/FT/2022/005). Financial support to the author YM by Fischer scholarship of the Faculty of Science, Palacky University in Olomouc in 2021. The authors would also like to express their gratitude to Mgr. Martin Pykala, PhD. (Catrin, Palacky University Olomouc) for preparation of graphical abstract.

Reference list

[1] A. Mishra and A. Gangele. Smart Materials For Clean And Sustainable Technology For Smart Cities, Materials Today-Proceedings. 2020 ;29:338-342

[2] J. Lv, Zhuoyu Liu, Jie Zhang, Jizhen Huo and Yingfeng Yu. Bio-based episulfide composed of cardanol/cardol for anti-corrosion coating applications, Polymer. 2017 ;121:286-296

[3] B. Hu. Biopolymer-based lightweight materials for packaging applications, Lightweight materials from biopolymers and biofibers. 2014:239-255

[4] R. Bourbonnais and Robert H. Marchessault. Application of polyhydroxyalkanoate granules for sizing of paper, Biomacromolecules. 2010 ;11:989-993

[5] L. Lapcik, B. Lapcikova and R. Zboril. Paper-based composite planar material,

[6] L. Lapcik, Petra Peterkova and Mihnea Gheorghiu. Method of increasing polypropylene biocompatibility by formation of a structured surface layer based on native or modified collagen, Czech Republic. 2004

[7] P. C. Nicolson, Richard Carlton Baron, Peter Chabrecek, et al. Extended wear ophthalmic lens, Official Gazette of the United States Patent and Trademark Office Patents. 2017

[8] P. Chabrecek and D. Lohmann. Surface modification of extended wear contact lenses by plasma-induced polymerization of vinyl monomers, Fundamental and Applied Aspects of Chemically Modified Surfaces. 1999:223-234. DOI:10.1533/9781845698591.223

[9] L. Lapcik, L. Lapcik, P. Kubicek, et al. Study of Penetration Kinetics of Sodium Hydroxide Aqueous Solution into Wood Samples, BioResources. 2014 ;9:881-893

[10] R. H. Marchessault. All things cellulose: a personal account of some historic events, Cellulose. 2011 ;18:1377-1379

[11] Z. Q. Shao and W. J. Wang. Structure and properties of cellulose nitrate, National Defense Industry Press, Beijing. 2011

[12] X. Zhang, Walid M. Hikal, Yue Zhang, et al. Direct laser initiation and improved thermal stability of nitrocellulose/graphene oxide nanocomposites, Appl.Phys.Lett. 2013 ;102:141905

[13] A. Li, Yadong Wang, Lijuan Deng, et al. Use of nitrocellulose membranes as a scaffold in cell culture, Cytotechnology. 2013 ;65:71-81

[14] X. Gao, Li-Ping Xu, Zhongxin Xue, et al. Dual-scaled porous nitrocellulose membranes with underwater superoleophobicity for highly efficient oil/water separation, Adv Mater. 2014 ;26:1771-1775

[15] Y. Zhang, Feijun Wang, Kezheng Gao, Yanhua Liu and Ziqiang Shao. Alcogel and aerogel of nitrocellulose formed in nitrocellulose/acetone/ethanol ternary system, International Journal of Polymeric Materials and Polymeric Biomaterials. 2016 ;65:377-383

[16] S. D. Dimitrijevich, Matthew Tatarko, Robert W. Gracy, Cary B. Linsky and Charles Olsen. Biodegradation of oxidized regenerated cellulose, Carbohydr.Res. 1990 ;195:247-256

[17] S. D. Dimitrijevich, Matthew Tatarko, Robert W. Gracy, et al. In vivo degradation of oxidized, regenerated cellulose, Carbohydr.Res. 1990 ;198:331-341

[18] R. L. Stilwell, M. G. Marks, L. Saferstein and D. M. Wiseman. Oxidized cellulose: chemistry, processing and medical applications, Drug Target.Recov.HandbookBiodegr.Polym. 1997 ;7:291-306

[19] V. Kumar and Tianrun Yang. HNO3/H3PO4–NANO2 mediated oxidation of cellulose—preparation and characterization of bioabsorbable oxidized celluloses in high yields and with different levels of oxidation, Carbohydr.Polym. 2002 ;48:403-412

[20] M. Bajerová, Kateřina Krejčová, Miloslava Rabišková, et al. Oxycellulose beads with drug exhibiting pH-dependent solubility, AAPS PharmSciTech. 2011 ;12:1348-1357

[21] P. Kanmani and Jong-Whan Rhim. Properties and characterization of bionanocomposite films prepared with various biopolymers and ZnO nanoparticles, Carbohydr.Polym. 2014 ;106:190-199

[22] A. Noreen, Khalid Mahmood Zia, Shazia Tabasum, et al. Hydroxyethylcellulose-g-poly (lactic acid) blended polyurethanes: Preparation, characterization and biological studies, Int.J.Biol.Macromol. 2020 ;151:993-1003

[23] P. Singh, Solange Magalhães, Luis Alves, et al. Cellulose-based edible films for probiotic entrapment, Food Hydrocoll. 2019 ;88:68-74

[24] J. R. Franca, Giselle Foureaux, Leonardo L. Fuscaldi, et al. Chitosan/hydroxyethyl cellulose inserts for sustained-release of dorzolamide for glaucoma treatment: In vitro and in vivo evaluation, Int.J.Pharm. 2019 ;570:118662

[25] O. V. Alekseeva, Anna N. Rodionova, Nadezhda A. Bagrovskaya, Alexandr V. Agafonov and Andrew V. Noskov. Effect of the bentonite filler on structure and properties of composites based on hydroxyethyl cellulose, Arabian journal of chemistry. 2019 ;12:398-404

[26] S. Tunç and Osman Duman. Preparation and characterization of biodegradable methyl cellulose/montmorillonite nanocomposite films, Appl.Clay.Sci. 2010 ;48:414-424

[27] M. Mikula, M. Čeppan, J. Blecha, L. Lapčík and V. Kalíšek. Kinetic dissolution measurement of polymers by solution viscosity recording, Polym.Test. 1988 ;8:339-351. DOI: https://doi.org/10.1016/0142-9418(88)90051-7

[28] V. Kalisek, L. Lapcik and B. Mikulaskova. Evaluation of the fixation of polyester based textile materials. III. Influence of the fixation conditions on swelling time and degree of fixation, Journal of Polymer Materials. 1998 ;15:299-309

[29] P. Pelikan, Michal Čeppan and Marek Liška. Applications of numerical methods in molecular spectroscopy (Fundamental & Applied Aspects of Chemometrics Book1 , 2020

[30] Ĺ Lapčík. Fotochemické procesy, 1989

[31] K. Liedermann, L. Lapčík and S. Desmedt. Study of the Molecular Mobility of Polysaccharide Solid Thin Layers by Dielectric Relaxation Spectroscopy, MRS Online Proceedings Library (OPL). 1997 ;500

[32] K. Liedermann and L. J. Lapcik. Dielectric relaxation spectroscopy of some polysaccharides, Chem.Pap. 1996 ;50:218-223

[33] P. Yu, Yufeng Hou, Hongjie Zhang, et al. Characterization and Solubility Effects of the Distribution of Carboxymethyl Substituents Along the Carboxymethyl Cellulose Molecular Chain, BioResources. 2019 ;14:8923-8934

[34] K. K. Mali, S. C. Dhawale, R. J. Dias, N. S. Dhane and V. S. Ghorpade. Citric acid crosslinked carboxymethyl cellulose-based composite hydrogel films for drug delivery, Indian Journal of Pharmaceutical Sciences. 2018 ;80:657-667

[35] R. N. Tirpude and Prashant K. Puranik. Rabeprazole sodium delayed-release multiparticulates: Effect of enteric coating layers on product performance, Journal of advanced pharmaceutical technology & research. 2011 ;2:184

[36] A. Kausar. Polymer coating technology for high performance applications: Fundamentals and advances, Journal of Macromolecular Science, Part A. 2018 ;55:440-448

[37] H. Choi, Hyungmin Park, Woong Sagong and Sang-im Lee. Biomimetic flow control based on morphological features of living creatures, Phys.Fluids. 2012 ;24:121302

[38] G. Marcelo, Enrique Saiz and M. Pilar Tarazona. Determination of molecular parameters of hydroxyethyl and hydroxypropyl celluloses by chromatography with dual detection, Journal of Chromatography A. 2007 ;1165:45-51

[39] J. Guo, G. W. Skinner, W. W. Harcum and P. E. Barnum. Pharmaceutical applications of naturally occurring water-soluble polymers, Pharm.Sci.Technol.Today. 1998 ;1:254-261. DOI: https://doi.org/10.1016/S1461-5347(98)00072-8

[40] C. G. Lopez, Ralph H. Colby and João T. Cabral. Electrostatic and hydrophobic interactions in NaCMC aqueous solutions: Effect of degree of substitution, Macromolecules. 2018 ;51:3165-3175

[41] C. Barba, Daniel Montané, Xavier Farriol, Jacques Desbrières and Marguerite Rinaudo. Synthesis and characterization of carboxymethylcelluloses from non-wood pulps II. Rheological behavior of CMC in aqueous solution, Cellulose. 2002 ;9:327-335

[42] C. G. Lopez and Walter Richtering. Oscillatory rheology of carboxymethyl cellulose gels: Influence of concentration and pH, Carbohydr.Polym. 2021 ;267:118117

[43] T. F. Liebert and Thomas J. Heinze. Exploitation of reactivity and selectivity in cellulose functionalization using unconventional media for the design of products showing new superstructures, Biomacromolecules. 2001 ;2:1124-1132

[44] L. Xiquan, Qu Tingzhu and Qi Shaoqui. Kinetics of the carboxymethylation of cellulose in the isopropyl alcohol system, Acta Polymerica. 1990 ;41:220-222

[45] G. Dürig and A. Banderet. Sur la structure des solutions aqueuses de carboxymethylcellulose, Helv.Chim.Acta. 1950 ;33:1106-1118

[46] E. H. DeButts, J. A. Hudy and J. H. Elliott. Rheology of sodium carboxymethylcellulose solutions, Industrial & Engineering Chemistry. 1957 ;49:94-98

[47] J. Hermans Jr. Investigation of the elastic properties of the particle network in gelled solutions of hydrocolloids. I. Carboxymethyl cellulose, Journal of Polymer Science Part A: General Papers. 1965 ;3:1859-1868

[48] L. G. Patruyo, A. J. Müller and A. E. Sáez. Shear and extensional rheology of solutions of modified hydroxyethyl celluloses and sodium dodecyl sulfate, Polymer. 2002 ;43:6481-6493

[49] A. C. Sau and Leo M. Landoll. Synthesis and solution properties of hydrophobically modified (hydroxyethyl) cellulose, 1989

[50] R. Tanaka, J. Meadows, P. A. Williams and G. O. Phillips. Interaction of hydrophobically modified hydroxyethyl cellulose with various added surfactants, Macromolecules. 1992 ;25:1304-1310

[51] U. Kästner, H. Hoffmann, R. Dönges and R. Ehrler. Hydrophobically and cationically modified hydroxyethyl cellulose and their interactions with surfactants, Colloids Surf.Physicochem.Eng.Aspects. 1994 ;82:279-297

[52] U. Kästner, H. Hoffmann, R. Dönges and R. Ehrler. Interactions between modified hydroxyethyl cellulose (HEC) and surfactants, Colloids Surf.Physicochem.Eng.Aspects. 1996 ;112:209-225

[53] S. Panmai. RK Prud homme, DG Peiffer, S. Jockusch, NJ Turro, Langmuir. 2002 ;18:3860-3864

[54] K. Thuresson, Svante Nilsson and Björn Lindman. Influence of cosolutes on phase behavior and viscosity of a nonionic cellulose ether. The effect of hydrophobic modification, Langmuir. 1996 ;12:2412-2417

[55] P. Rachtanapun, Suwaporn Luangkamin, Krittika Tanprasert and Rungsiri Suriyatem. Carboxymethyl cellulose film from durian rind, LWT-Food Science and Technology. 2012 ;48:52-58

[56] P. Rachatanapun and N. Rattanapanone. Synthesis and characterization of carboxymethyl cellulose from Mimosa Pigra peel, J Appl Polym Sci. 2011 ;122:3218-3226

[57] D. Wahyuningtyas and Arwitra Dinata. Combination of carboxymethyl cellulose (CMC)-Corn starch edible film and glycerol plasticizer as a delivery system of diclofenac sodium, 2018 ;1977:030032

[58] Z. Lu, Jizhen Huang, E. Songfeng, et al. All cellulose composites prepared by hydroxyethyl cellulose and cellulose nanocrystals through the crosslink of polyisocyanate, Carbohydr.Polym. 2020 ;250:116919

[59] A. Khan, Ruhul A. Khan, Stephane Salmieri, et al. Mechanical and barrier properties of nanocrystalline cellulose reinforced chitosan based nanocomposite films, Carbohydr.Polym. 2012 ;90:1601-1608

[60] T. Huq, Stephane Salmieri, Avik Khan, et al. Nanocrystalline cellulose (NCC) reinforced alginate based biodegradable nanocomposite film, Carbohydr.Polym. 2012 ;90:1757-1763

[61] I. Kassem, Zineb Kassab, Mehdi Khouloud, et al. Phosphoric acid-mediated green preparation of regenerated cellulose spheres and their use for all-cellulose cross-linked superabsorbent hydrogels, Int.J.Biol.Macromol. 2020 ;162:136-149

[62] M. Kirsch, Luise Birnstein, Iliyana Pepelanova, et al. Gelatin-methacryloyl (GelMA) formulated with human platelet lysate supports mesenchymal stem cell proliferation and differentiation and enhances the hydrogel's mechanical properties, Bioengineering. 2019 ;6:76

[63] R. M. Barrer. Some properties of diffusion coefficients in polymers, J.Phys.Chem. 1957 ;61:178-189

[64] N. Mourougou-Candoni, B. Prunet-Foch, F. Legay, M. Vignes-Adler and K. Wong. Influence of dynamic surface tension on the spreading of surfactant solution droplets impacting onto a low-surface-energy solid substrate, J.Colloid Interface Sci. 1997 ;192:129-141

[65] L. Lapčík 1963-. Gelová forma hmoty jako základ materiálově-inženýrských prvků : teze přednášky k profesorskému jmenovacímu řízení v oboru Materiálové vědy a inženýrství, 2002

[66] R. L. Thompson. Solvent-free polymer lithography via the Kirkendall effect, Nuclear Instruments and Methods in Physics Research Section B: Beam Interactions with Materials and Atoms. 2010 ;268:2181-2184

[67] H. Abou-Yousef and Samir Kamel. High efficiency antimicrobial cellulose-based nanocomposite hydrogels, J Appl Polym Sci. 2015 ;132

[68] L. Lapčík, L. Valko, M. Mikula, V. Jančovičová and J. Panak. Kinetics of swollen surface layer formation in the diffusion process of polymer dissolution, 1988:221-226

[69] K. Ueberreiter. u. F. Asmussen: J, Polymer Sci. 1957 ;23:75

[70] V. K. Ueberreiter and Frithjof Asmussen. Die auflösungsgeschwindigkeit von polymeren. 1. Formulierung des vorganges und seine temperaturabhängigkeit, Die Makromolekulare Chemie: Macromolecular Chemistry and Physics. 1961 ;44:324-337

[71] V. F. Asmussen and Kurt Ueberreiter. Die auflösungsgeschwindigkeit von polymeren, 2. Mitteilung. Untersuchung der stabilität der quellschicht durch konzentrationsund viskositätsmessungen, Die Makromolekulare Chemie: Macromolecular Chemistry and Physics. 1962 ;52:164-173

[72] K. Ueberreiter and Frithjof Asmussen. Velocity of dissolution of polymers. Part I, Journal of Polymer Science. 1962 ;57:187-198

[73] F. Asmussen and Kurt Ueberreiter. Velocity of dissolution of polymers. Part II, Journal of Polymer Science. 1962 ;57:199-208

[74] F. Asmussen and Kurt Ueberreiter. Die Auflösungsgeschwindigkeit von Polymeren, Kolloid-Zeitschrift und Zeitschrift für Polymere. 1968 ;223:6-13

[75] V. K. Ueberreiter and Peter Kirchner. Die auflösungsgeschwindigkeit von polymeren. 4. Mitt. Der einfluß der strömung des lösungsmittels, Die Makromolekulare Chemie: Macromolecular Chemistry and Physics. 1965 ;87:32-59

[76] M. Pisarcik, M. Mikula, D. Mariianiova and L. Lapcik. The influence of hydroxyethylcellulose on the diffusion of acetylsalicylic-acid trihydromagnesium salt in aqueous-solution, Acta Polymerica. 1993 ;44:92-96. DOI: 10.1002/actp.1993.010440206

[77] P. Peterkova and L. Lapcik. Determination of the diffusion coefficient of water into atelocollagen type I thin films by attenuated total reflection Fourier transform infrared spectroscopy, Colloid Polym.Sci. 2000 ;278:1014-1016. DOI: 10.1007/s003960000366

[78] R. H. Xiong, H. Deschout, J. Demeester, S. C. De Smedt and K. Braeckmans. Rectangle FRAP for Measuring Diffusion with a Laser Scanning Microscope, 2014 ;1076:433-441. DOI: 10.1007/978-1-62703-649-8_18; 10.1007/978-1-62703-649-8

[79] Y. Wu, Sony Joseph and N. R. Aluru. Effect of cross-linking on the diffusion of water, ions, and small molecules in hydrogels, The Journal of Physical Chemistry B. 2009 ;113:3512-3520

[80] J. Jamlang, Mica Therese Marañon, Girro Jonn Rigor and Terence Tumolva. Developing a physically cross-linked hydroxyethyl cellulose hydrogel for wound dressing applications, 2019 ;947:3-12

[81] B. Ghanbarzadeh, Hadi Almasi and Ali A. Entezami. Physical properties of edible modified starch/carboxymethyl cellulose films, Innovative food science & emerging technologies. 2010 ;11:697-702

[82] Y. Seki, Aylin Altinisik, Başak Demircioğlu and Caner Tetik. Carboxymethylcellulose (CMC)–hydroxyethylcellulose (HEC) based hydrogels: synthesis and characterization, Cellulose. 2014 ;21:1689-1698

[83] J. M. Joshi and Vijay Kumar Sinha. Graft copolymerization of 2-hydroxyethylmethacrylate onto carboxymethyl chitosan using CAN as an initiator, Polymer. 2006 ;47:2198-2204

[84] P. K. Pandey, Arti Srivastava, Jasaswini Tripathy and Kunj Behari. Graft copolymerization of acrylic acid onto guar gum initiated by vanadium (V)–mercaptosuccinic acid redox pair, Carbohydr.Polym. 2006 ;65:414-420

[85] S. J. Metz, WJC Van de Ven, Jens Potreck, MHV Mulder and Matthias Wessling. Transport of water vapor and inert gas mixtures through highly selective and highly permeable polymer membranes, J.Membr.Sci. 2005 ;251:29-41

[86] F. Soleimani, Hossein Sadeghi, Hadis Shahsavari, Arezou Soleimani and Fatemeh Sadeghi. Studies of swelling kinetics of carboxymethyl cellulose-g-PMAAm-co-PNIPAm superabsorbent hydrogels, Asian Journal of Chemistry. 2013 ;25:4851

[87] W. Wang, Jiang Wang, Yuru Kang and Aiqin Wang. Synthesis, swelling and responsive properties of a new composite hydrogel based on hydroxyethyl cellulose and medicinal stone, Composites Part B: Engineering. 2011 ;42:809-818

[88] H. Schott. Swelling kinetics of polymers, Journal of Macromolecular Science, Part B: Physics. 1992 ;31:1-9

[89] V. Kalisek, L. Lapcik and B. Mikulaskova. Evaluation of the fixation of polyester based textile materials. III. Influence of the fixation conditions on swelling time and degree of fixation, Journal of Polymer Materials. 1998 ;15:299-309

[90] A. Mracek, K. Benesova, A. Minarik, P. Urban and L. Lapcik. The diffusion process of sodium hyaluronate (Na-HA) and Na-HA-n-alkyl derivatives films swelling, Journal of Biomedical Materials Research Part A. 2007 ;83A:184-190. DOI: 10.1002/jbm.a.31188

[91] K. Ueberreiter. Diffusion in polymers, Diffusion in Polymers. 1968

[92] L. Lapcik, A. Machackova, A. Minarik, et al. The Internal Pressure in Thin Polymer Layers in Contact with Liquids, 41.Mezinárodní konference o nátěrových hmotách, KNH 2010. 2010:27-36

[93] H. Drnovska and Lubomir Jr Lapcik. Hyaluronate derivatives and their applications, Plasty Kauc. 1999 ;36:291-294

[94] L. Lapcik, L. Lapcik, S. De Smedt, J. Demeester and P. Chabrecek. Hyaluronan: Preparation, structure, properties, and applications, Chem.Rev. 1998 ;98:2663-2684. DOI: 10.1021/cr941199z

[95] K. A. Uyanga, Oghenefego P. Okpozo, Okwuchi S. Onyekwere and Walid A. Daoud. Citric acid crosslinked natural bi-polymer-based composite hydrogels: Effect of polymer ratio and beta-cyclodextrin on hydrogel microstructure, React Funct Polym. 2020 ;154:104682

[96] I. Kupska, L. Lapcik, B. Lapcikova, K. Zakova and J. Jurikova. The viscometric behaviour of sodium hyaluronate in aqueous and KCl solutions, Colloids and surfaces: A-physicochemical and engineering aspects. 2014 ;454:32-37. DOI: 10.1016/j.colsurfa.2014.04.018

[97] B. Lapcikova, T. Valenta and L. Lapcik. Rheological Properties of Food Hydrocolloids based on Polysaccharides, Journal of Polymer Materials. 2017 ;34:631-645

[98] P. V. Toledo, Diego PC Limeira, Nicolas C. Siqueira and Denise FS Petri. Carboxymethyl cellulose/poly (acrylic acid) interpenetrating polymer network hydrogels as multifunctional adsorbents, Cellulose. 2019 ;26:597-615

[99] M. Raab. Materiály a člověk:(netradiční úvod do současné materiálové vědy), 1999

[100] L. Lapcik, D. Bakos and V. Kello. Transannular peroxides of anthracene and its derivatives. Preparation, properties, applications. Chem.Listy. 1990 ;84:582-605

[101] A. Stasko, A. Blazkova, V. Brezova, M. Breza and L. Lapcik. Oxygen photosenzitization in the presence of sodium anthracene-1-sulfonate, Journal of Photochemistry and Photobiology A-Chemistry. 1993 ;76:159-165. DOI: 10.1016/1010-6030(93)80132-S

[102] L. Lapcík, Barbora Lapcíková and Andrej Stasko. EPR Study of the Thermal Decomposition of Transannular Peroxide of Anthracene, International Journal of Organic Chemistry. 2011 ;1:37

[103] A. Maleki, Anna-Lena Kjøniksen and Bo Nyström. Effect of shear on intramolecular and intermolecular association during cross-linking of hydroxyethylcellulose in dilute aqueous solutions, The Journal of Physical Chemistry B. 2005 ;109:12329-12336

[104] A. Maleki, Anna-Lena Kjøniksen and Bo Nyström. Effect of shear on intramolecular and intermolecular association during cross-linking of hydroxyethylcellulose in dilute aqueous solutions, The Journal of Physical Chemistry B. 2005 ;109:12329-12336

[105] L. Lapcik, K. Benesova, L. Lapcik, S. de Smedt and B. Lapcikova. Chemical modification of hyaluronic acid: Alkylation , International journal of polymer analysis and characterization. 2010 ;15:486-496. DOI: 10.1080/1023666X.2010.520904

Figure chapter

Fig. 1 (a) Chemical structure of cellulose; (b) Chemical structure of carboxymethyl cellulose with its sodium salt; (c) Chemical structure of hydroxyethyl cellulose

Fig. 2 Analysis of the tensile strength (Reproduced from ref. [57] with the permission of American Institute of Physics licence no. 5270921480448)

Fig. 3 Analysis of the percentage elongation (Reproduced from ref. [57] with the permission of American Institute of Physics licence no. 5270921480448)

Fig. 4 Spreading factor versus time for water and each surfactant at critical micellar concentration (CM conc × 10) (Reproduced from ref. [64] with the permission of Academic Press, Elsevier Science licence no. 5270931090431)

Fig. 5 Structure of the swollen surface layer by Ueberreiter K. and F. Asmussen: δ_1 - liquid layer, δ_2 - rubbery layer, δ_3 - gel layer, δ_4 - infiltration layer, T - temperature of sloughing, T_L - temperature of phase transition of solvent, T_{gel} - gelling temperature, T_g - glass transition temperature, and T_F - melting temperature of polymer (Reproduced from [69, 72, 74])

Fig. 6 Surface swollen layer of (a) CMC and (b) HEC (1 cm ~ 0.1mm) (Reproduced from ref. [68] with the permission of Springer Nature licence no. 5274210286515

Fig. 7 Water uptake of HEC hydrogel samples with respect to time (Reproduced from ref. [80] with the permission of Trans Tech Publications Ltd. Request ID 600074454)

Fig. 8 Moisture absorption of starch films as a function of CMC content (Reproduced from ref. [81] with permission from Elsevier licence no. 5274220418935

Fig. 9 Representative swelling kinetics of the CMC-g-PMAAm-coPNIPAAm superabsorbent hydrogel with various particle sizes (Courtesy of [86])

Fig. 10 Plot *t*/*W* vs. time according to equation 12 (second - order kinetics) for superabsorbent hydrogels with various particle sizes (Courtesy of [86])

Fig. 11 (a) swelling kinetic curves of the hydrogels (MS dosage, 0, 5, 10 and 50 wt%) in distilled water, (b) effect of the saline solution with various concentration on the kinetic swelling behaviours of the composite hydrogel (MS dosage, 10 wt%), and (c) effect of particle size on the kinetic swelling behaviours of the composite hydrogel (MS dosage, 10 wt%) (Adapted from ref. [87] with request from Elsevier request ID 600074472)

Fig. 12 Distribution of the polymer concentration in the swollen layer δ composed from δ_1 - liquid, δ_2 - rubbery, δ_3 - solid swollen and δ_4 - infiltration layers in a distance from the interface at different mixing rates v_i ($v_2 > v_1 > v_0 = 0$), φ – volume fraction of the polymer (courtesy of [89])

Fig. 13 Mechanism of the cross-linker reaction and schematic representation of intra- and inter-polymer cross-linking [103] Reprinted with permission from Atoosa Maleki, Anna-Lena Kjøniksen, Bo Nyström: “Effect of Shear on Intramolecular and Intermolecular Association during Cross-Linking of Hydroxyethylcellulose in Dilute Aqueous Solutions”; The Journal of Physical Chemistry B, 109 (Jun 1) 12329-12336 (2005). Copyright 2005 American Chemical Society.

Table chapter

Table 1.

Parameter	Compound	
	CMC	**HEC**
$10^3 (\varepsilon_s - \varepsilon_\infty)$	37.60	2.28
	2.18	
α	0.0598	0.676
	0.970	
β	1.000	1.000
	1.000	
$10^{-3}\ \tau_0$/s	68.100	5.120
	3.810	
A'	2.48×10^{-19}	1.08×10^{-18}
n	0.700	0.535

ε_∞ optical permittivity of the sample, ε_s static permittivity of the sample, $(\varepsilon_s - \varepsilon_\infty)$ relaxation strength, τ_0 position of the relaxation on the same axis, α slope of the low – frequency side of the relaxation curve, product $\alpha \times \beta$ describes the slope of the high – frequency side of the relaxation curve, *A'* is sample surface area, and *n* is purely D.C. conductivity mechanism.

Table 2.

Degrees of substitution (DS)	Mean length (mm)	Mean width (µm)	Percentage crystallinity (%)	Purity (%)
0.75	2.28	48.1	18.03	95
0.76	2.13	55.7	19.60	95
0.80	1.94	52.8	23.51	95
0.73	1.43	51.7	25.85	95

Table 3.

Types of film	Tensile strength (MPa)	Elongation at break (%)
20g/100mL NaOH-CMC	141.16 ± 8.32	2.32 ± 0.26
30g/100mL NaOH-CMC	255.54 ± 4.13	2.20 ± 0.81
40g/100mL NaOH-CMC	140.77 ± 14.43	2.07 ± 0.50
50g/100mL NaOH-CMC	53.42 ± 8.21	2.95 ± 1.13
60g/100mL NaOH-CMC	79.62 ± 9.76	2.28 ± 0.98

Table 4.

Surfactant	CMC (g/litre)	Equilibrium surface tension at CM conc × 10 (mN/m)
NPOEOP	0.06	36.9
C13OE18	0.08	27.7
Silvett L77	0.10	20.4
C10OE6	0.80	26.1
TTAB	1.18	37.2
CTAC	0.42	34
DOS	0.92	27
SDS	2.38	36.5
SDG	0.60	25

NPOEOP: nonylphenyl polyoxypropylene; C13OE18: isodecyl polyoxyethylene; Silvett L77: trisilioxane oxypropylene polyoxyethylene; C10OE6: isodecyl polyoxyethylene; TTAB: tetradecyl trimethylammonium bromide; CTAC: cetyltrimethylammonium chloride; DOS: sodium dioctyl sulfosuccinate; SDS: sodium dodecyl sulfate; SDG: sodium decylgalacturonate

Table 5.

	12.5% HEC	**13.75% HEC**	**15.0 % HEC**
% Maximum Water Uptake	160.5	173.8	156.9

Graphical abstract

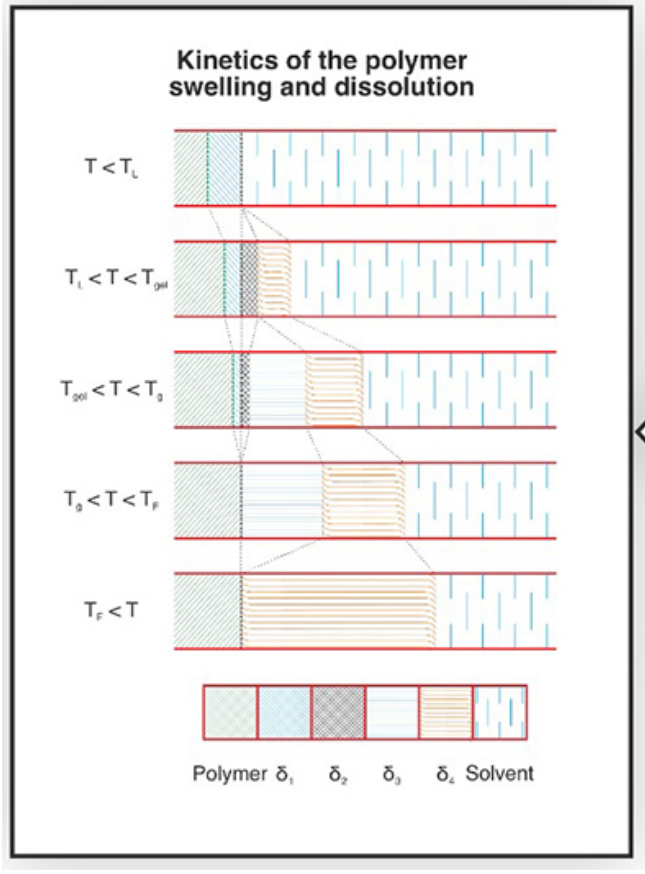

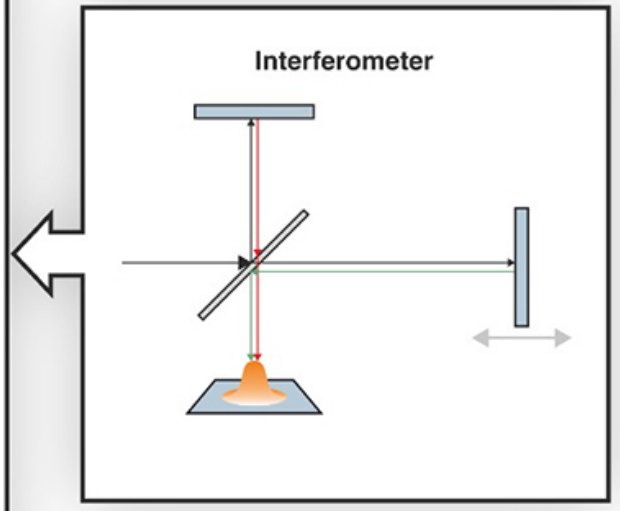

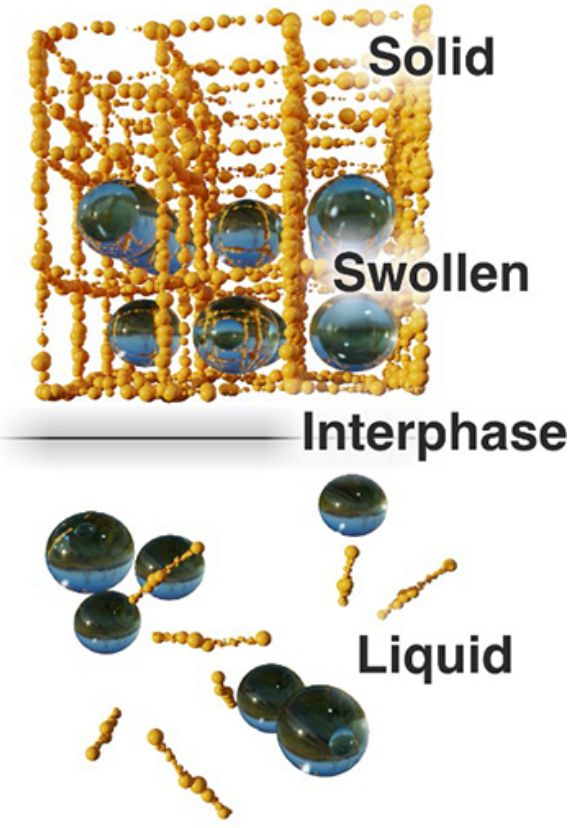

Graphics Abstract

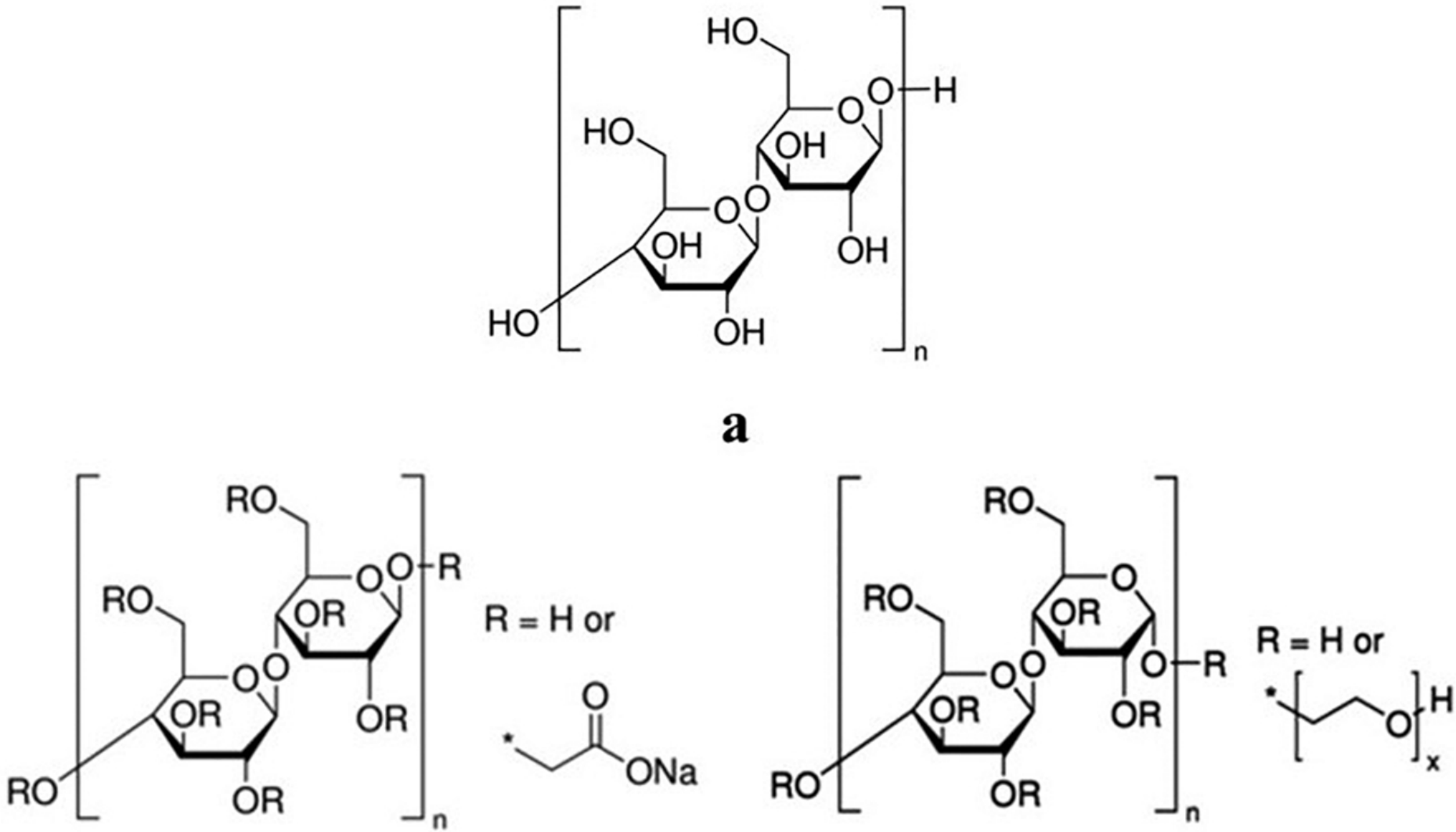
HO
HO
OH
O
O
H
HO
OH
OH
HO
OH
n
a
RO
RO
OR
O
O
R
OR
OR
RO
OR
n
R = H or
O
ONa
b
RO
RO
OR
O
O
R
OR
OR
RO
OR
n
R = H or
H
x
c

Figure 1

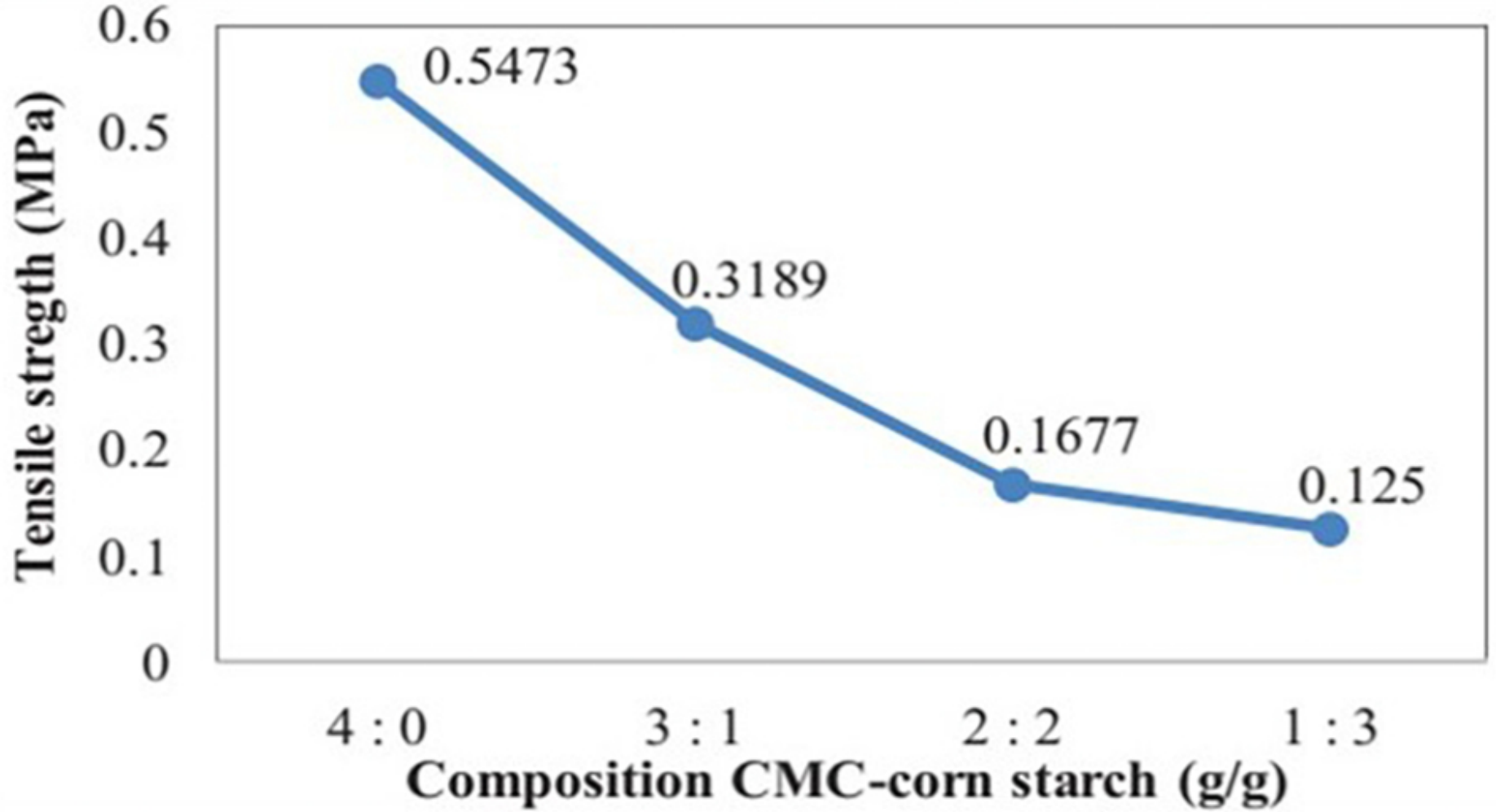
0.6
0.5
0.4
0.3
0.2
0.1
0
Tensile stregth (MPa)
0.5473
0.3189
0.1677
0.125
4 : 0
3 : 1
2 : 2
1 : 3
Composition CMC-corn starch (g/g)

Figure 2

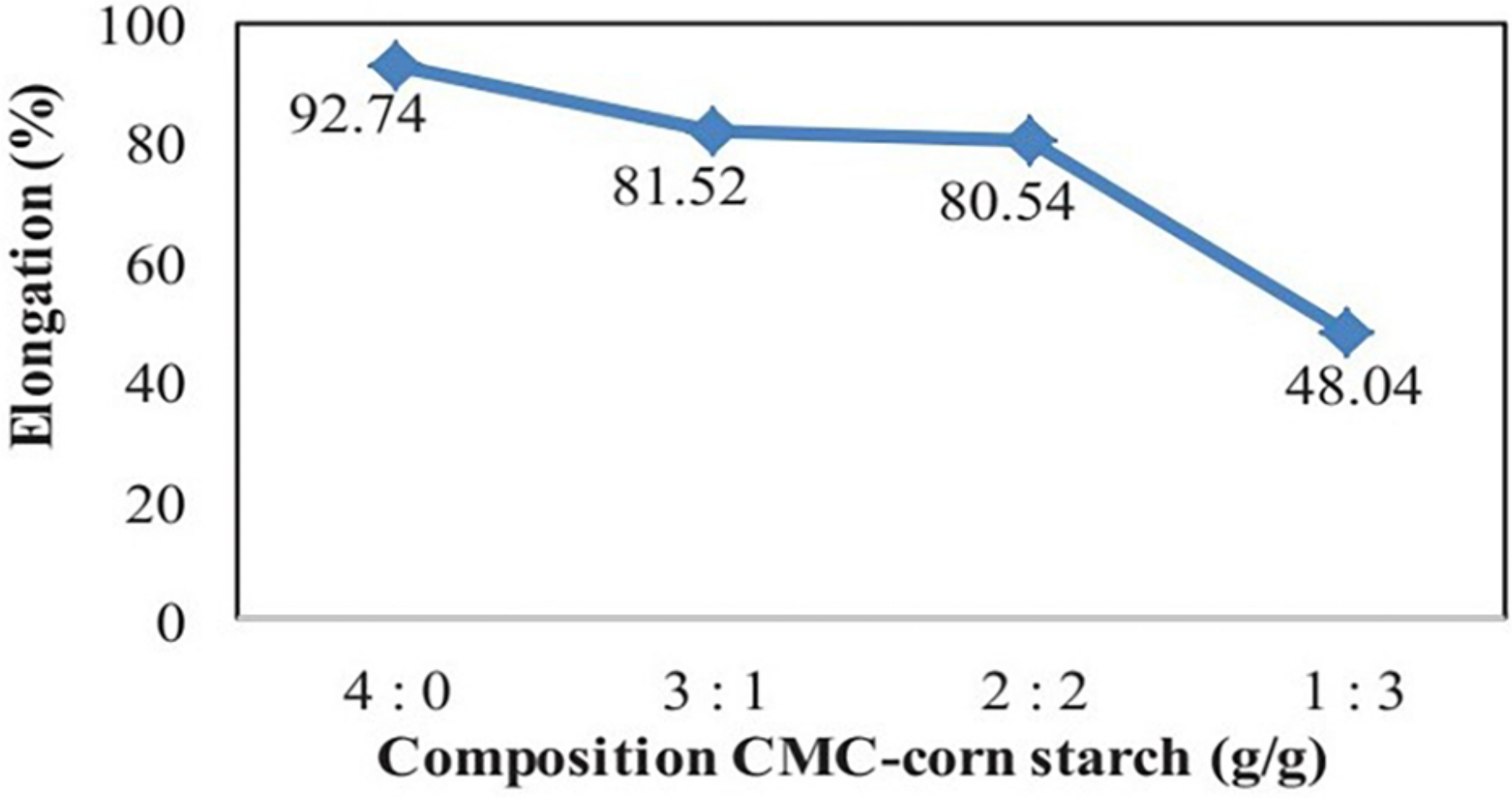
100
80
60
40
20
0
Elongation (%)
92.74
81.52
80.54
48.04
4 : 0
3 : 1
2 : 2
1 : 3
Composition CMC-corn starch (g/g)

Figure 3

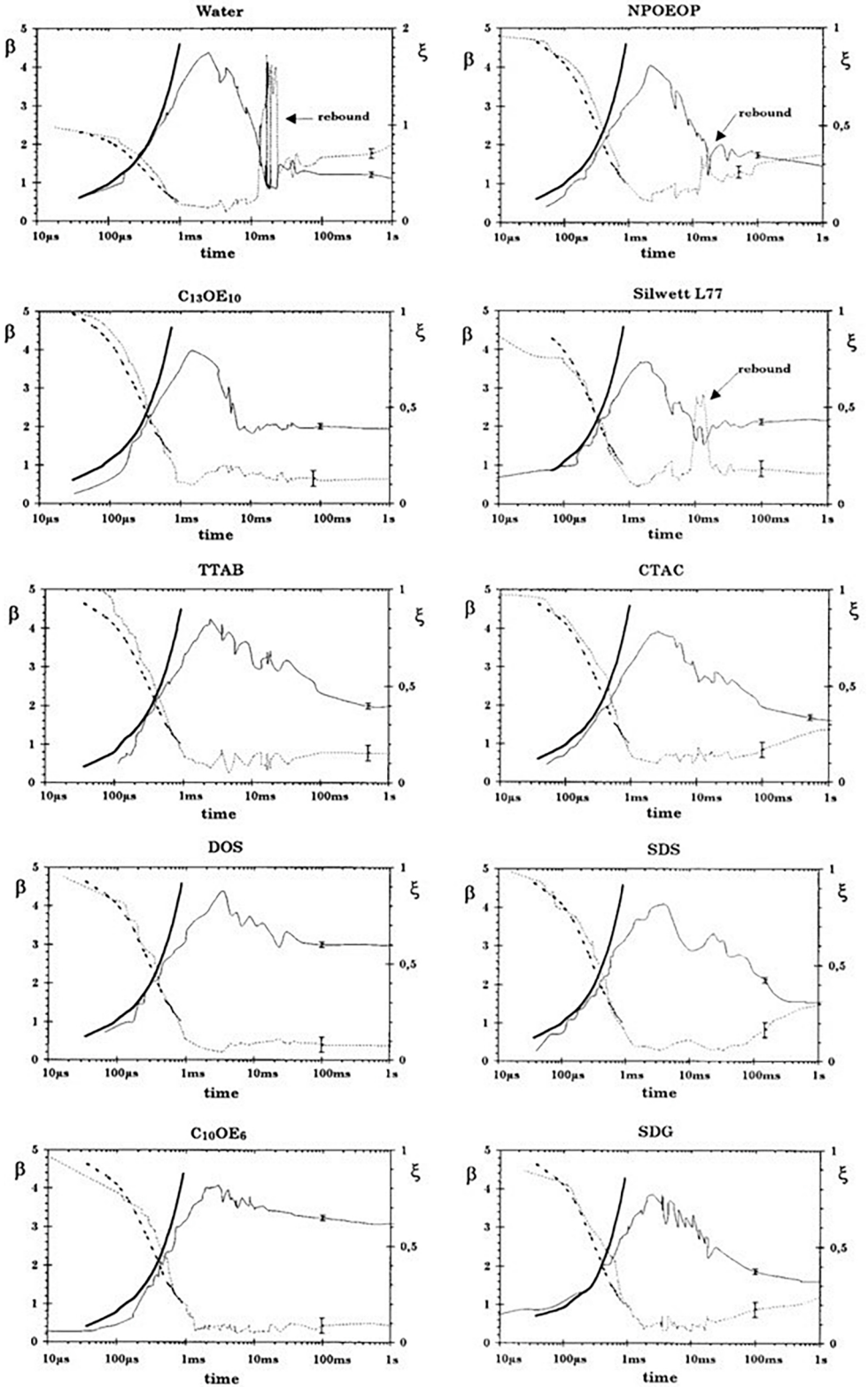
Water
rebound
NPOEOP
rebound
C13OE10
Silwett L77
rebound
TTAB
CTAC
DOS
SDS
C10OE6
SDG
β
ξ
time
10µs
100µs
1ms
10ms
100ms
1s

Figure 4

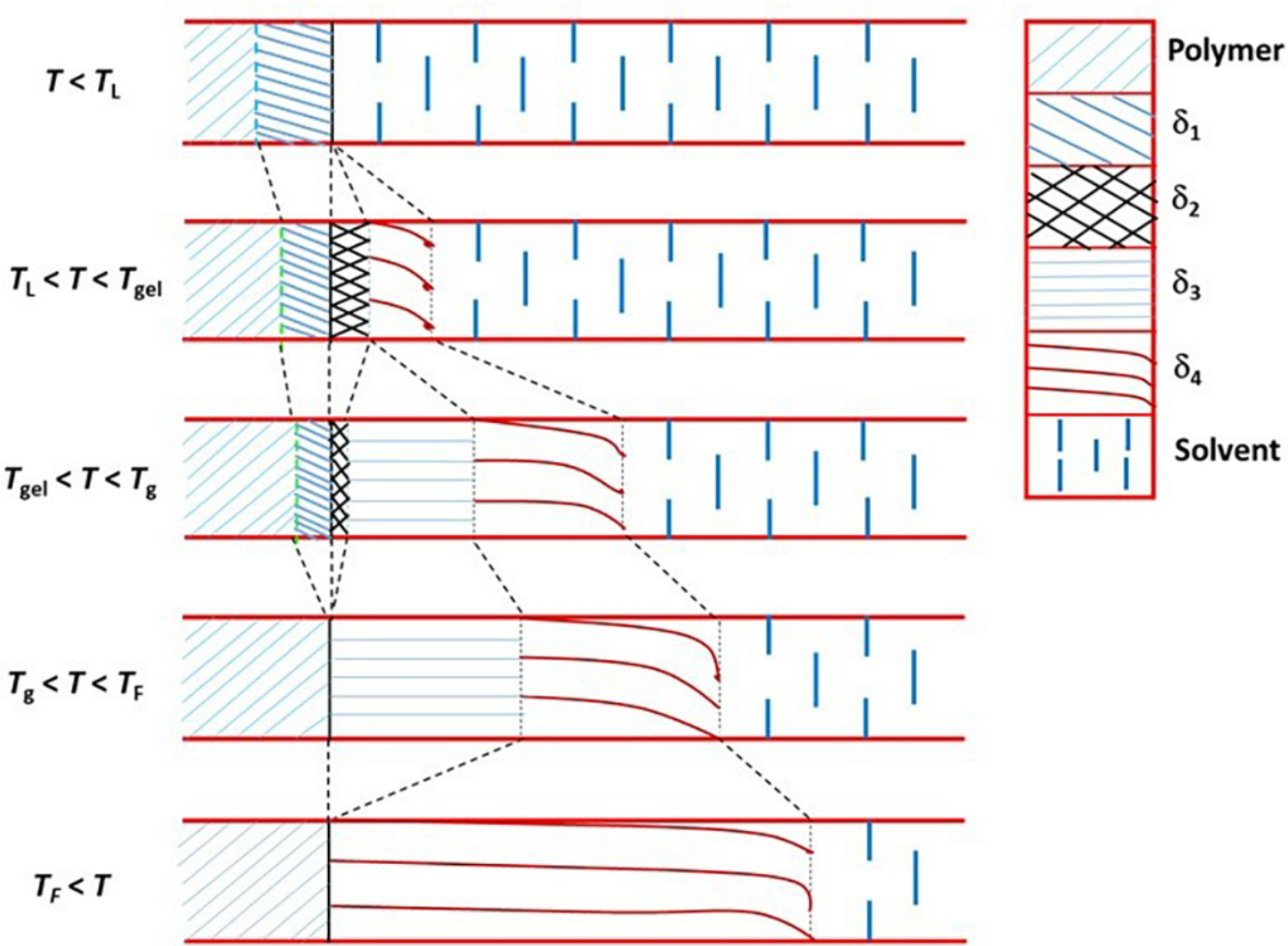
$T < T_L$
$T_L < T < T_{gel}$
$T_{gel} < T < T_g$
$T_g < T < T_F$
$T_F < T$
Polymer
δ_1
δ_2
δ_3
δ_4
Solvent

Figure 5

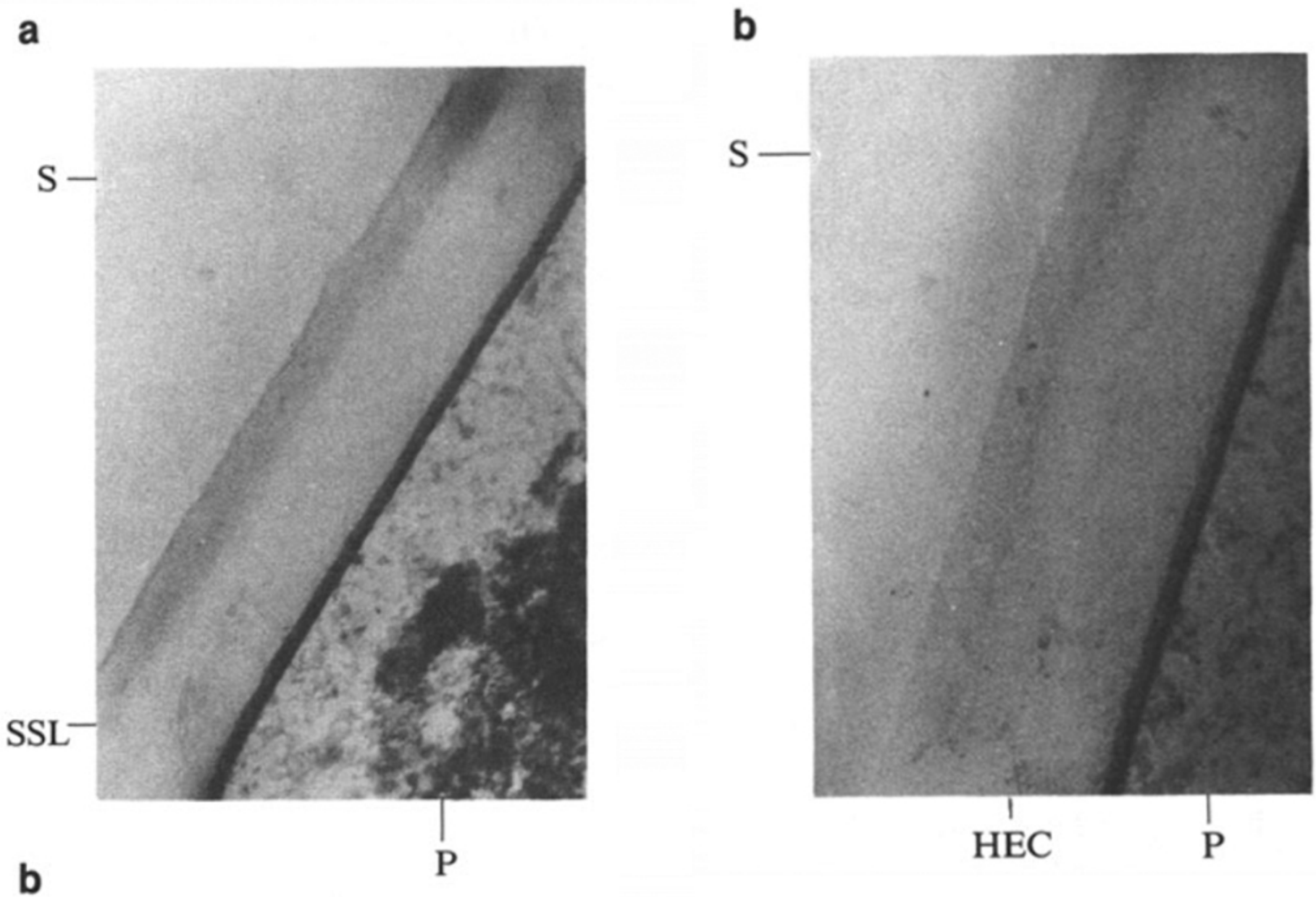

Figure 6

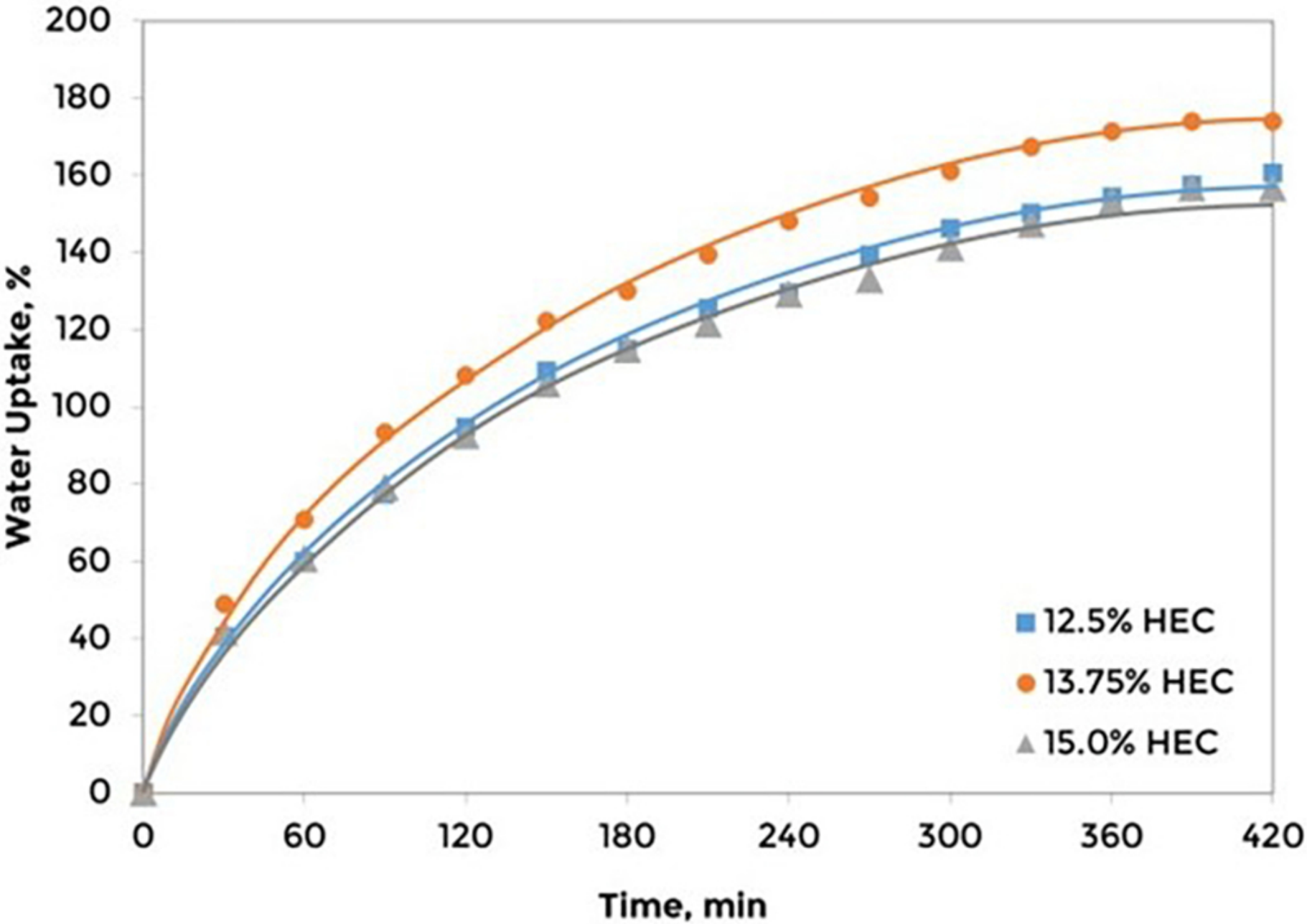
Water Uptake, %
200
180
160
140
120
100
80
60
40
20
0
0
60
120
180
240
300
360
420
Time, min
12.5% HEC
13.75% HEC
15.0% HEC

Figure 7

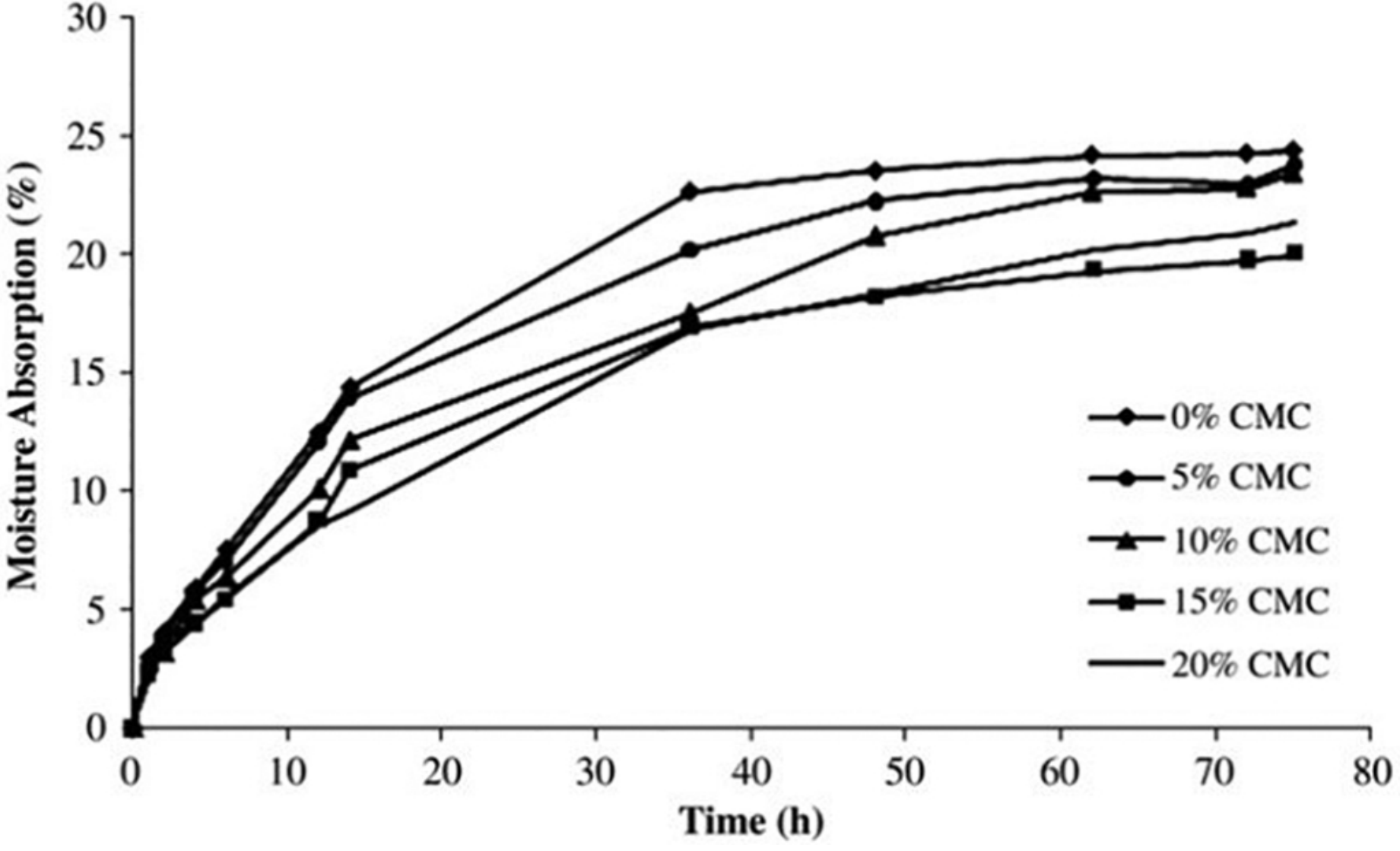
Moisture Absorption (%)
30
25
20
15
10
5
0
0
10
20
30
40
50
60
70
80
Time (h)
0% CMC
5% CMC
10% CMC
15% CMC
20% CMC

Figure 8

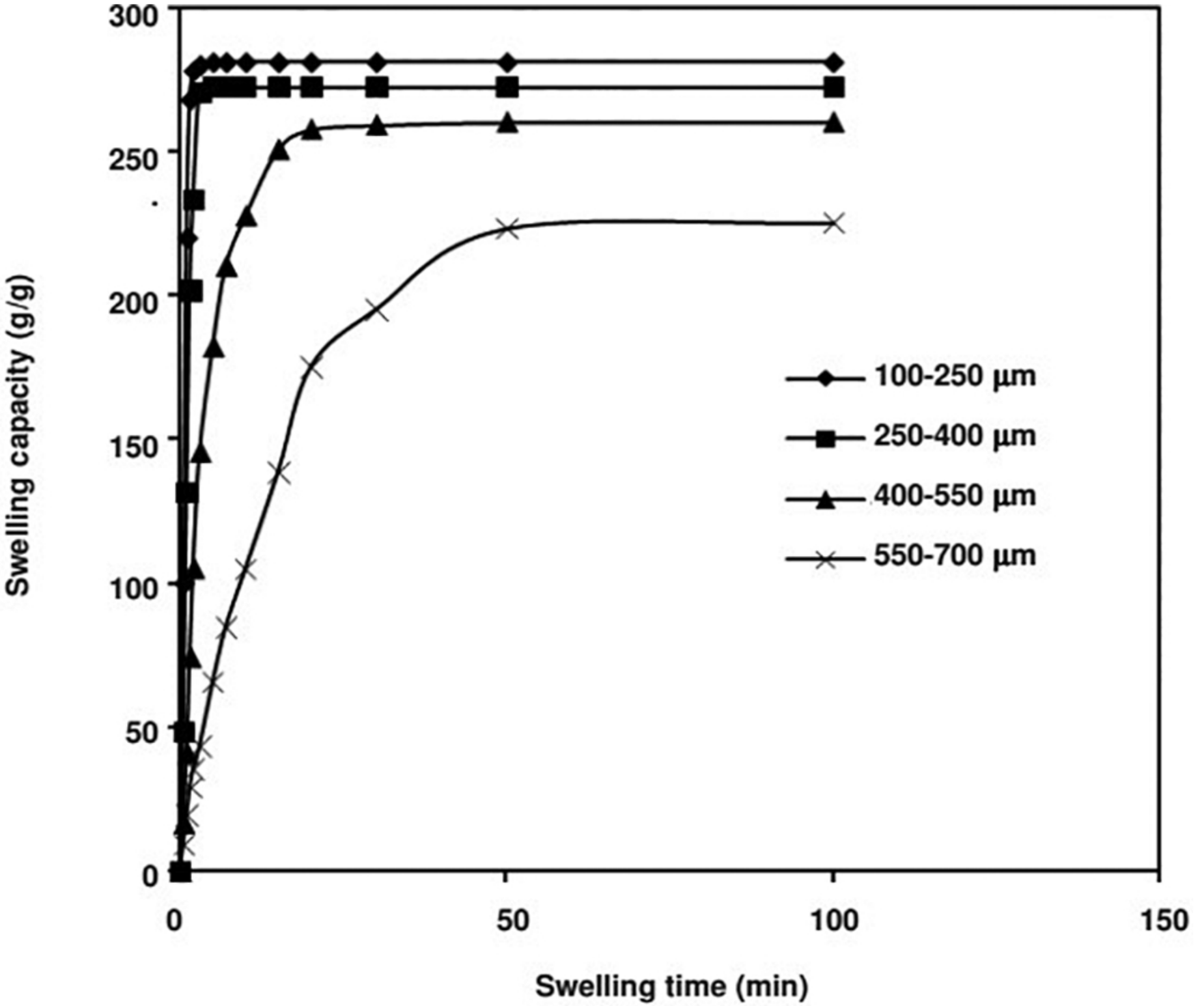
300
250
200
150
100
50
0
Swelling capacity (g/g)
0
50
100
150
Swelling time (min)
100-250 µm
250-400 µm
400-550 µm
550-700 µm

Figure 9

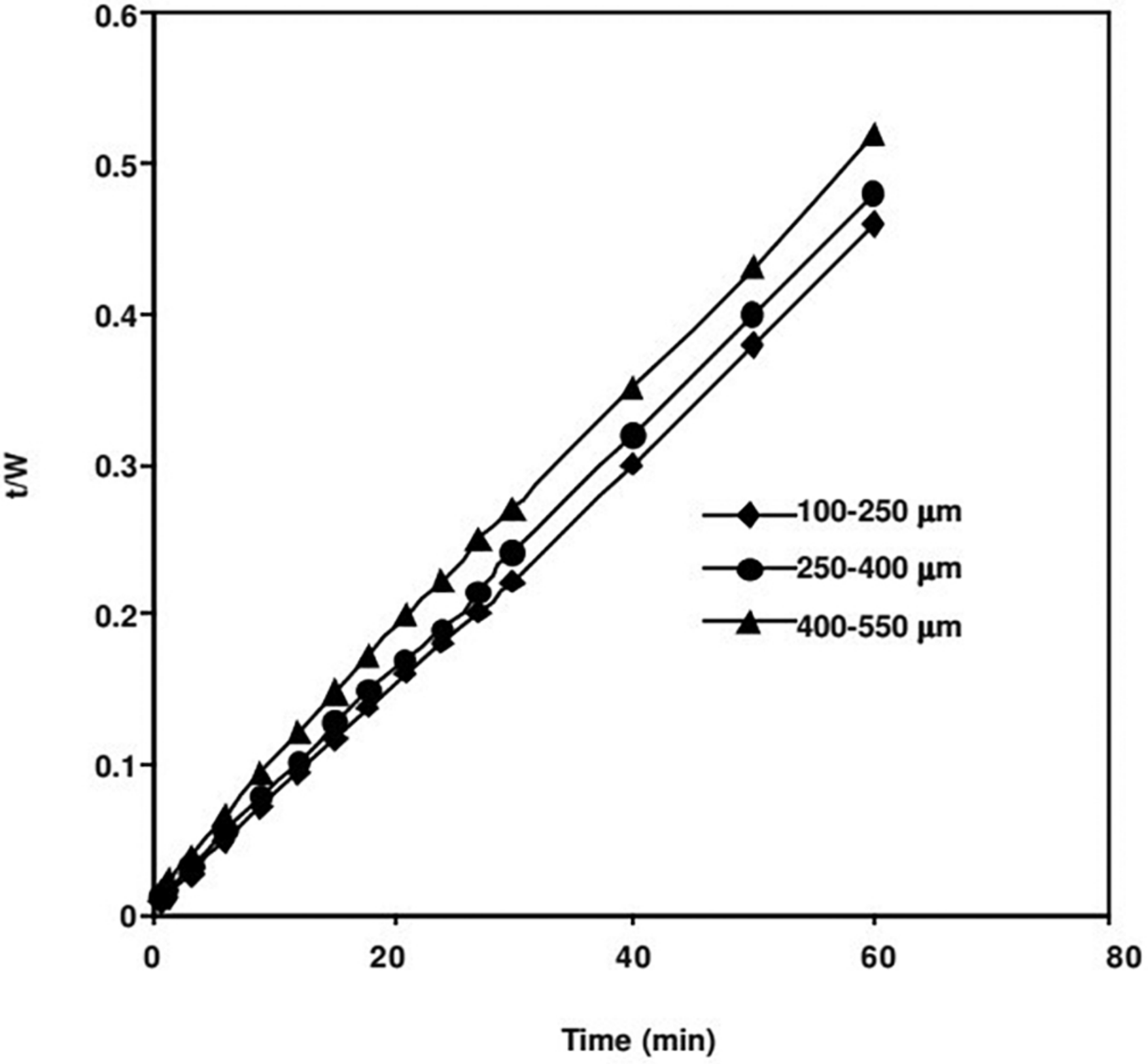
0.6
0.5
0.4
0.3
0.2
0.1
0
t/W
0
20
40
60
80
Time (min)
100-250 µm
250-400 µm
400-550 µm

Figure 10

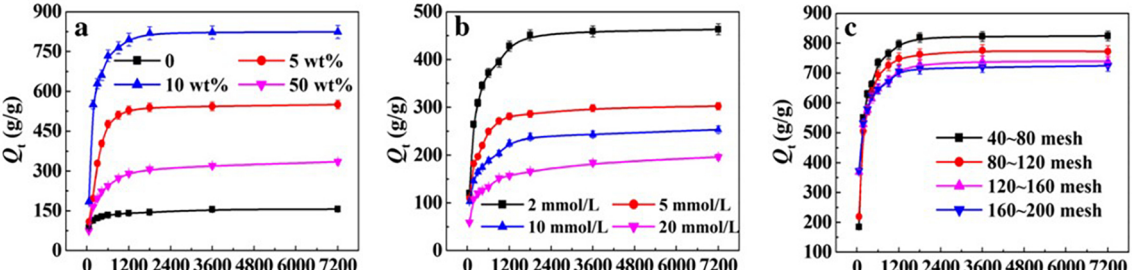
a
b
c
Q_t (g/g)
0
5 wt%
10 wt%
50 wt%
2 mmol/L
5 mmol/L
10 mmol/L
20 mmol/L
40~80 mesh
80~120 mesh
120~160 mesh
160~200 mesh
0 1200 2400 3600 4800 6000 7200

Figure 11

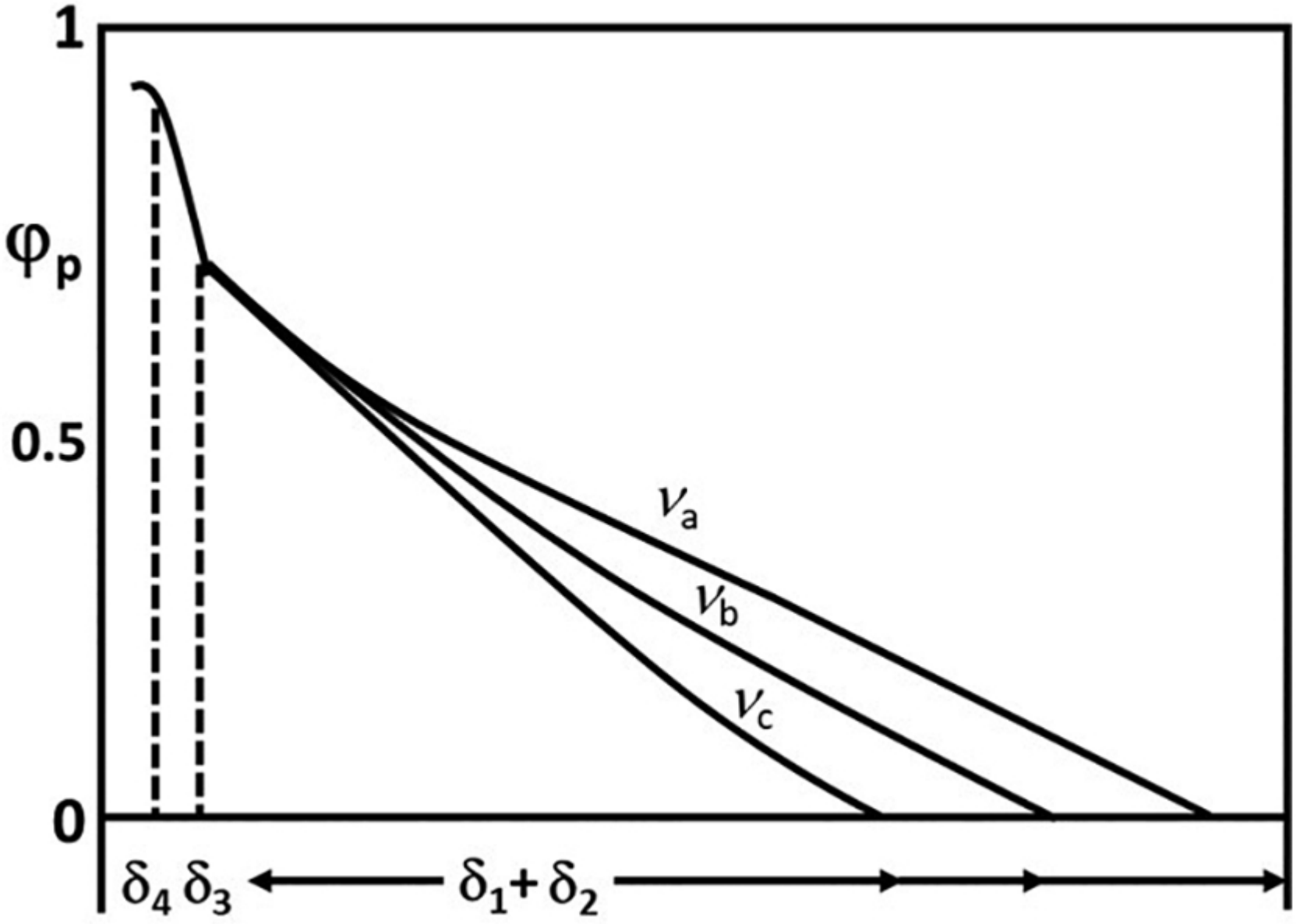

Figure 12

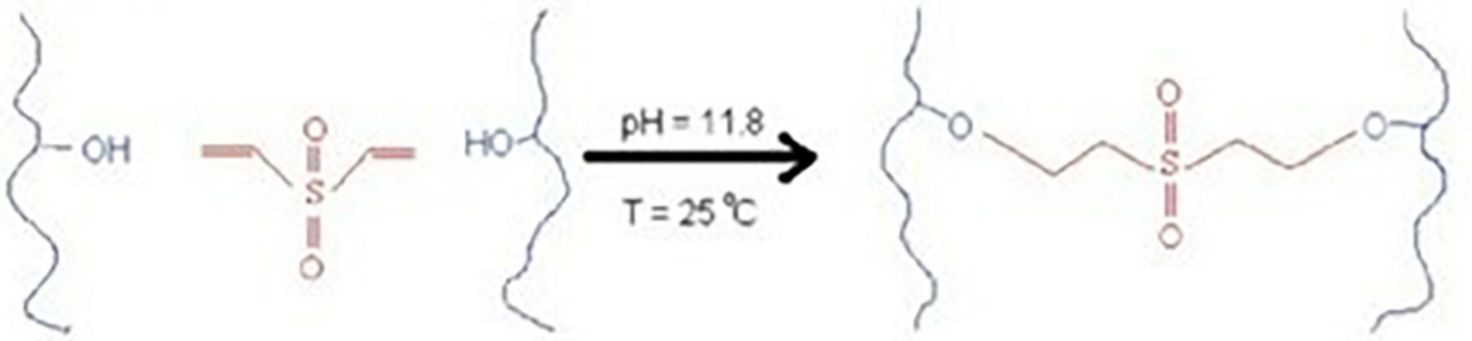

Intermolecular cross-linked polymer

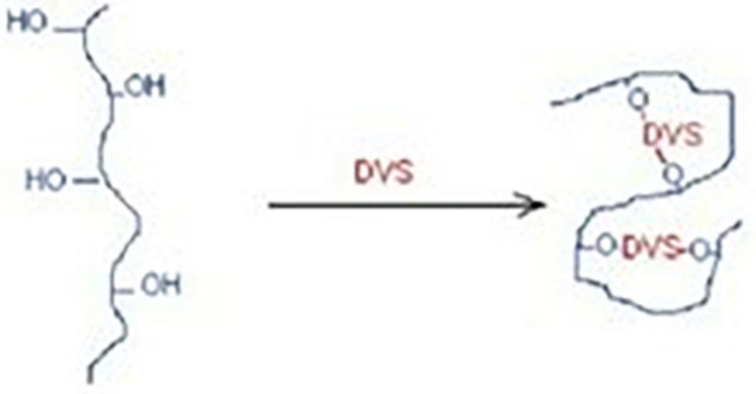

Intramolecular cross-linked polymer

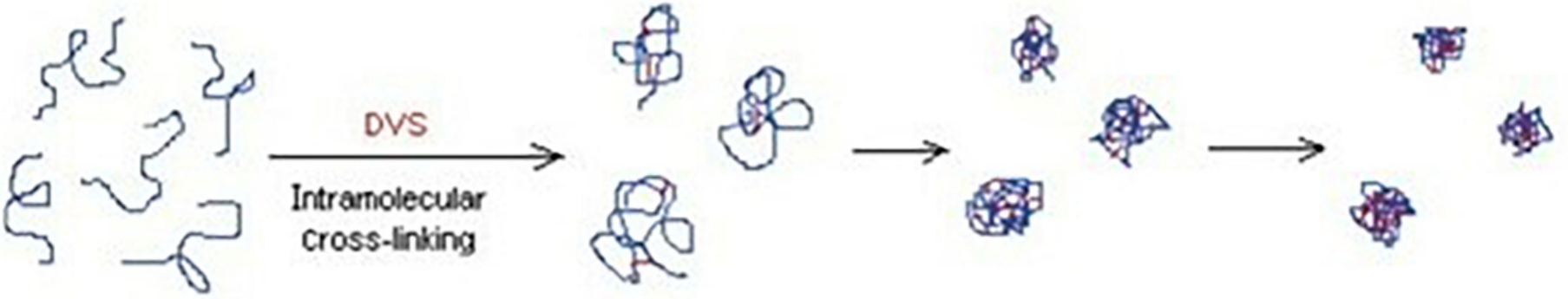

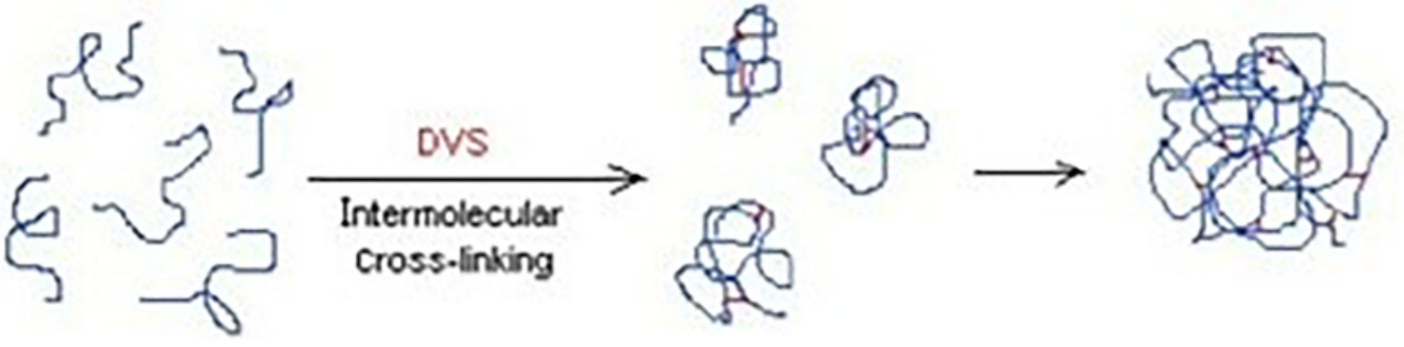

Figure 13